Biocomposite of sodium-alginate with acidified clay for wastewater treatment: Kinetic, equilibrium and thermodynamic studies

Kausar, A., Sher, F., Hazafa, A., Javed, A., Sillanpää, M. & Iqbal, M.

Biocomposite of sodium-alginate with acidified clay for wastewater treatment: Kinetic, equilibrium and thermodynamic studies

Abida Kausar[1], Farooq Sher[2,*], Abu Hazafa[3], Anum Javed[1], Mika Sillanpää[4,5,6] and Munawar Iqbal[7,*]

[1]Department of Chemistry, Government College Women University, Faisalabad 38000, Pakistan
[2]School of Mechanical, Aerospace and Automotive Engineering, Faculty of Engineering, Environment and Computing, Coventry University, Coventry CV1 5FB, UK
[3]Department of Biochemistry, University of Agriculture, Faisalabad, 38000, Pakistan
[4]Institute of Research and Development, Duy Tan University, Da Nang 550000, Vietnam
[5]Faculty of Environment and Chemical Engineering, Duy Tan University, Da Nang 550000, Vietnam
[6]School of Civil Engineering and Surveying, Faculty of Health, Engineering and Sciences, University of Southern Queensland, West Street, Toowoomba, 4350 QLD, Australia
[7]Department of Chemistry, The University of Lahore, Lahore 53700, Pakistan

*Corresponding author:
E-mail: Farooq.Sher@coventry.ac.uk (F. Sher); Tel: +44 (0) 24 7765 7688

Abstract

Clay-based composites were prepared, characterized, and applied for the elimination of Blue FBN (BFBN) and Rose FRN (RFRN) dyes. The Fourier transform infrared spectroscopy (FTIR), scanning electron microscope (SEM), Thermogravimetric (TGA) and X-ray diffraction analyses were performed to check the interaction of dye molecule with adsorbents. The analysis showed a successful interaction between adsorbent and dyes ions. The experimental data was best fitted with Freundlich isotherm for both dyes (BFBN and RFRN). The findings revealed that at 80 min the adsorption grasped equilibrium in the case of both dyes and succeeded in the pseudo-second-order kinetics model. Furthermore, the enthalpy ($\Delta H°$), Gibbs free energy ($\Delta G°$) and entropy ($\Delta S°$) change suggested that adsorption was exothermic, physical and spontaneous in nature. The maximum adsorption capacities were determined as 76.39% for BFBN and 59.85% for RFRN dye at pH 2.0 and 30 °C. Composites found to be stable at a higher temperature and regenerated using

MgSO$_4$ eluting agent. The textile effluent colour was removed up to 50.35 and 54.95% using raw and modified clay, respectively. The modified clay showed promising efficiency for adsorption of synthetic BFBN and RFRN dyes from aqueous solution, which could be a viable option for the treatment of industrial wastewater and textile effluents.

Keywords: Biocomposites; Raw-modified clay; Cationic-anionic dyes; Adsorption-desorption; Stability-regeneration and Ionic-anionic dyes.

1. Introduction

Recently, the remediation of wastewater using modified materials gained much attention [1-9]. In the past few decades, different types of adsorbents including ashes, agro-industrial wastes and activated carbon have been examined for the removal of pollutants from wastewater [10-14]. Nevertheless, due to low adsorption capacity, slow adsorption kinetics, disposal problems, cost and regeneration difficulty, these adsorbents did not attain much attention. On the other hand, clay offered efficient, affordable and eco-benign to combat the pollution issue [15-18]. Moreover, the composites are stable and showed enhanced physic-chemical properties [19]. Clay has been investigated as the most significant adsorbent because of its strong sorption complexation ability [20]. Recently, different types of clays including; montmorillonite [21], bentonite [22], expanded vermiculite [23] and natural illicit clay mineral [24] have been experimentally examined for the adsorption of different types of pollutants [25, 26]. The phyllosilicates are abundantly present in clay that induce the plasticity when it becomes dry. Clay materials are characterized depending on differences in layered structures. Hence, the use of clays has attracted many researchers due to a number of advantages, like easy accessibility, affordable cost, eco-benign, high surface area and much potential for ion exchange [27]. Combination of clay with different materials like manganese

oxide [28], polyacrylamide-bentonite complex with amine functionality (Am-PAA-B) [29], TiO_2-kaolinite nanocomposites and modified natural bentonite clay using cetyl trimetyl-ammonium bromide showed promising efficiency and offered as an effective way to develop adsorbents [16]. Clay is a commonly found material that can easily be picked and comprehend the mechanism of dye removal as an adsorbent [26].

Dye containing waste is one of the major sources of water contamination. Dyes are coloured organic compounds that are made up of two main components, namely chromophores (e.g., NR_2, NHR, NH_2, COOH, and OH) and auxochromes (e.g., N_2, NO, and NO_2). The chromophore is a colour importing substance, which is the base of acidic, basic, azo, vat, reactive and disperses dyes [30-33]. Each dye has wide employment in different fields such as plastic, paper, carpet, food, printing, cosmetic and textile industries. Globally, > 10,000 tons of dyes are consumed by the textile industry per year that are released in effluents (10–15%) during dyeing processes [34-37]. The dyes present in effluents are considered toxic. Most recently, genotoxic and mutagenic effects have been reported in model organisms that were exposed to dyes and effluents containing dyes [38-40]. Since the last century, chemists have been investigating how to synthesize a plethora of new products including synthetic dyes. Synthetic dyes have provided many bright hues, but these are causing a major threat of environmental pollution. The textile industry yields a huge amount of consumed dye baths that are lethal, carcinogenic and therefore, constitute serious harms to all kinds of life [41-44]. The synthetic dyes are composed of complex aromatic rings that give colour strength to the dyes and making their metabolic products lethal and non-biodegradable when discharged into wastes [39, 40]. To date, different techniques have been investigated for the degradation of dye, which can be classified as chemical (e.g., fenton reagent, ozonation, and

photocatalyst), biological (e.g., aerobic and anaerobic degradation) and physicochemical methods (e.g., ion exchange, adsorption, and membrane filtration). However, due to high cost, less separation efficiency and design these methods have received less attention [45-52]. The emerging evidence suggested that adsorption is the most important separation method at an industrial level for the treatment of wastewater. In the adsorption method, dissolved constituents can be selectively eliminated from aqueous solution through solid substances (adsorbent) by attaching the dissolved solute at their surface. The adsorbent can be a gas, liquid, solid or dissolved solute phase [10, 15, 17, 18, 20]. According to emerging evidences the clay is considered as low-cost adsorbent because it contains high adsorption capacity due to its greater surface area. Besides, clays carry a net negative charge on silicate minerals that are neutralized by the positive charge of cationic dyes. Studies also showed that the adsorption capacity of clays can be enhanced by modification [16, 18, 25, 26].

Based on the aforementioned facts, the present investigation is focused on local raw and modified clay as an adsorbent to propose a cheap adsorbent for the adsorption of blue FBN and rose FRN dyes. The reusability of adsorbents was also assessed. Further, the interaction of adsorbate and adsorbent surface was investigated by advanced techniques. The retention of dye stuff was examined under different conditions such as initial pH, temperature, dye concentration, and contact time. Finally, the optimum conditions were applied for the adsorption of dyes from textile effluents.

2. Material and methods

2.1. Materials

The clay was obtained from Best Way Cement Hattar industry (KPK, Pakistan) having a composition as; SiO_2 (49–52%), Fe_2O_3 (5–6%), Al_2O_3 (10–12%), MgO (2.70–2.80%), CaO (8–8.5%), K_2O (2–2.30%), SO_3 (0.02%), Na_2O (1.00%), and K_2O (2–2.30%). The blue functionalized boron nitride (BFBN) and Rose-FRN dyes were purchased from Masood Textile Mills, Faisalabad, Pakistan. To form a homogeneous solution of uniform size, the adsorbent clay was wash-down, dried, grounded, sieved and stored in desiccators until further use. Other analytical graded chemicals including; H_2SO_4, HCl, EDTA, NaOH, $MgSO_4.7H_2O$, Cu $(NO_3)_2.3H_2O$, $Pb(NO_3)_2$, $CdCO_3$, $NiSO_4.7H_2O$, sodium dodecyl sulphate (SDS) and sodium alginate were purchased from SIGMA-Aldrich (USA). Furthermore, Octagon Siever (OCT-Digital 4527-01), orbital incubator shaker, analytical balance (Shimadzu AW-220), ultra-centrifuge (80-3), pH meter (Adwa AD-8000), grinder (Moulinex, France), thermal electric thermostatic drying oven (DHG-9030A) and double beam spectrophotometer (UV/VIS. 2800 -EZTECH) were used in the present study.

2.2. Preparation of adsorbents

A 0.5 M HCl was added into raw clay with a ratio of 1:10 (g/mL) at 30 $^{\circ}$C and agitated at 120 rpm in an orbital incubator shaker. Then, the acid-treated clay (acidified clay) showered numerous times with deionized water. Finally, the mixture was centrifuged and dried at 55 $^{\circ}$C for 12 h and stored in a desiccator until further use [53]. To form uniform beads of an immobilized adsorbent, 2.0 g/100 mL sodium-alginate was dissolved in distilled water by heating as precisely followed by a method of Bayramoglu and Arica [54]. After cooling, the adsorbent (1 g/100 mL) was mixed with this slurry and stirred to mix it properly. Then, the alginate-adsorbent slurry was moulded

into uniform beads using 0.1 M CaCl$_2$. After washing with distilled water, beads were stockpiled in 0.05 M CaCl$_2$ solution at 4 °C. For the treatment of raw clay with sodium dodecyl sulphate (SDS), the clay powder (0.5 g) was mixed in 50 mL distilled water as reported by Fan et al. [55]. A solution was prepared by dissolving 0.44 mmol of SDS in 80 mL distilled water and this mixture was added into the clay at 70 °C. Then, this clay dispersion was kept for 12 h at room temperature and subjected to an ultrasonic bath at 70 °C for 1 h. Finally, it was filtered and washes with deionized water. The attained acidified clay was ground into a powder after drying in a vacuum at 70 °C for 12 h.

For the preparation of stock solutions of both BFBN and RFRN dyes, 1 g of dye was dissolved in 1 L of double deionized water and further dilution was made to prepare different concentrations (10–100 mg/L). Furthermore, UV/vis spectrophotometry was used to calculate the absorbance of both dyes' solutions. A 0.1 g of each adsorbent (raw, acidified, immobilized and SDS treated clay) was mixed in 250 mL of conical flasks (contain 50 mL of 100 mg/L BFBN/RFRN dyes solution at 2 pH) for screening. After screening, the solutions were shaken for 2 h with a speed of 125 rpm then, centrifuged and filtered. BFBN and RFRN containing filtrates were analysed by the spectrophotometric method.

2.3. Characterization

The scanning electron microscopy (SEM JSM-5910, JEOL), X-Ray Diffraction (Bruker D8: XRD), surface area analysis (BET), thermogravimetric analysis (TGA) and Fourier transform infrared spectroscopy (Shimadzu, IR Prestigue-21: FTIR) was used to characterize the adsorbents. BET (Brunauer, Emmett and Teller) was accomplished on the surface area of analyser (NOVA 2200, Quanta Chrome, USA with nitrogen standard) to examine the adsorbents (raw and acidified

clay), while JEOL (JSM-5910) was applied for the determination of the composition. Similarly, SEM analyses were carried out on each sample by using Pt coating that inhibits the charge indulgence during its scanning at 10 kV in an Argon atmosphere. Thermal analysis was conducted in a nitrogen atmosphere using Perkin Elmer Pyris 1, at 5 °C/min under nitrogen flow rate 20 mL/min and the temperature was ramped from 40 to 800 °C. All samples (loaded and unloaded) were recorded in a FTIR-8400S (Shimadzu) from the percentage transmittance versus wavenumber in the range of 4,000–6500 cm^{-1}, resolution 2 cm^{-1} and 32 scans, Bio-Rad Merlin software was used to record the spectra.

2.4. Adsorption experiment

2.4.1. Adsorption of BFBN and RFRN onto raw and acidified clays

The batch adsorption technique was investigated to find the equilibrium information necessary to analyse the chemistry of adsorbent and dye. Screening results of different adsorbents (raw, acidified, immobilized and SDS treated) showed that raw and acidified clay is the most optimal adsorbent for both BFBN and RFRN dyes. The equilibrium adsorption capacities of both dyes were obtained using Eq. 1.

$$q_e = (C_o - C_e) \, V/W \qquad\qquad (1)$$

where, C_o is the initial dye concentration, C_e is the equilibrium dye concentration, V is the volume of the solution (L) and W is the mass of adsorbent (g). Similarly, the percentage of removal was examined using Eq. 2.

$$\text{Removal} (\%) = (C_o - C_e)100/C_o \tag{2}$$

The experiments were performed to determine the optimum pH of both BFBN and RFRN dyes by adding 0.05 g/25 mL of adsorbent at pH 2–12 with 25 mg/L of initial dye concentration. The dependence of adsorption on the adsorbent quantity of both dyes was investigated by using different amounts (0.05–0.25 g/25 mL for both BFBN and RFRN solutions) of raw and acidified clay. Furthermore, the dependence of adsorption on the equilibrium time was studied using adsorbent (0.05 g/25 mL) in each dye solution (25 mg/L) at a shaking speed of 125 rpm and 30 °C. A 0.05 g of adsorbent was mixed with the solution of both dyes to perform dye concentration analysis using different initial dye concentrations and the temperature outcome was examined in the range of 30–50 °C. Finally, the adsorption measurements were analysed by shaking the solution for 2 h at 125 rpm and at an optimum temperature (30 °C) and pH (2). For the calculation of point of zero charge (pH$_{pzc}$), the solid addition process is considered as the most precise method [1, 2]. For this, a series of 50 mL of 0.1 M NaCl solutions were prepared in the pH range of 2 to 12. For pH adjustments, 0.1 M HCl and NaOH were used. A 0.03 g of adsorbent was mixed in all of these solutions and suspensions were shaken intermittently. A graph between ΔpH versus initial pH was made and point of zero charge (pH$_{pzc}$) was obtained at the intersection of the curve [1, 2].

2.4.2. Adsorption kinetics

The pseudo-first and second-order kinetic models were applied to interpret the experimental findings. A statistical representation of the linear form of pseudo-first kinetic model is displayed in Eq. 3 [56].

$$\log(q_e - q_t) = \log(q_e) - \frac{k_1}{2.303}t \tag{3}$$

where q_e and q_t represent volumes of dyes adsorbed (mg/g) at equilibrium and at time t (min) respectively and k_1 pseudo-first-order rate constant (1/min). To find the rate of k_1 the plot of $\log(q_e - q_t)$ was compared with t. Linear pseudo-second orders kinetics model expression is presented in Eq. 4 [57].

$$\frac{t}{q_t} = \frac{1}{K_2 q_e^2} + \left(\frac{1}{q_e}\right) t \tag{4}$$

where q_e and q_t represent dyes adsorbed (mg/g) at equilibrium and at time t (min) respectively and k_2 is the pseudo-second-order rate constant (g/mg min).

2.4.3. Adsorption isotherms

The adsorption isotherms are very important to determine the adsorption capacity and to characterize the adsorption process, which signifies the association between the absorption of dyes (BFBN and RFRN) and the amount of sorbate adsorbed. In this regard, a linear regression analysis was found to be efficient for the equilibrium model. The linear Freundlich equation is expressed in Eq. 5 [58].

$$\log(q_e) = \log(K_F) + \frac{1}{n} \log(C_e) \tag{5}$$

where, K_F and $1/n$ are calculated from the intercept and slope, respectively in the linear regression method. Langmuir model evaluates monolayer adsorption. The mathematical representation of the Langmuir model is described in Eq. 6 [59].

$$\frac{C_e}{q_e} = \frac{1}{q_m} Ce + \frac{1}{K_a q_m} \tag{6}$$

where q_e represents the amount of dyes sorbed (mg/g) at equilibrium, q_m is maximum adsorption capacity (mg/g), Ce is the equilibrium concentration of dyes (mg/L) and K_L is adsorption equilibrium constant (L/mg). Usually, a straight line is observed between C_e/q_e versus Ce plot. The Redlich-Peterson isotherm model is another significant model that does not pursue the ideal monolayer adsorption and combines elements from both Freundlich and Langmuir isotherms as shown in Eq. 7. Where B (mg/L) and g are Redlich-Peterson coefficients and can be calculated from $\ln\left(A\frac{C_e}{q_e} - 1\right)$ versus $\ln(C_e)$.

$$\ln\left(A\frac{C_e}{q_e} - 1\right) = g\ln(C_e) + \ln(B) \tag{7}$$

2.4.4. Desorption and thermodynamic studies

The desorption studies were performed to regenerate the adsorption that made a treatment process more economical. To regenerate the adsorbent and check its reusability, desorption studies were performed using different eluting agents, namely HCl, $MgSO_4$, H_2SO_4 and NaOH. The BFBN and RFRN dyes (0.05 g/25 mL) were desorbed under an optimized condition to generate adsorbent then dyes loaded adsorbents were dried for 24 h at 40 °C in the oven. Finally, the raw and acidified clays were desorbed in 0.1 M 50 mL solution of each eluting agent by continuously shaking at 125 rpm for 1 h. The Eqs. 8-9 were used to calculate the percentage desorption and desorption amount respectively.

$$\text{Desorption (\%)} = \left[\frac{q_{des}}{q_{ads}}\right]100 \tag{8}$$

$$q_{des} = C_{des}\,{}^V\!/_W \tag{9}$$

where q_{des} is eluted dye amount (mg/g) and C_{des} (mg/ L) is dye concentration in eluent solution of volume V (L) and W is the weight of adsorbent (g). The thermodynamics parameters including; ΔS^o, ΔG^o and ΔH^o were computed as shown in Eqs. 10-11.

$$\Delta G^\circ = \Delta H^\circ - T \Delta S^o \qquad (10)$$

$$Log\ (q_e/C_e) = -\Delta H^o/2.303RT + \Delta S^o/2.303R \qquad (11)$$

2.5. Effect of interfering ions

The effect of different cations like Ni^{2+}, Pb^{2+}, Cd^{2+}, and Cu^{2+} (5, 10 and 15 mg/L of each ion) was evaluated on both dyes (25 mg/L) adsorption onto raw and acidified clay under optimized conditions.

2.6. Application of optimum conditions to treat textile effluent

Real textile wastewater samples were collected from Masood Textile Mills, Faisalabad in sampling bottles. The effluent was diluted as; 10, 20 and 30 times. The experiments were conducted under optimum conditions of process variables and Eq. (2) was used for the estimation of percentage colour removal.

3. Results and discussion

3.1. Characterization of adsorbents

3.1.1. Fourier transforms infrared (FTIR) analysis

To understand the surface characteristics [60] of raw and acidified clay FTIR analysis was carried out before and after adsorption of both BFBN and RFRN dyes. **Fig. 1** represents the FTIR spectra of acidified loaded and unloaded clay with BFBN dye. During the FTIR study, a number of peaks were observed, that indicated a complex structure of unloaded and loaded raw and acidified clay (**Fig. 1**) The spectra of raw clay (unloaded and loaded with BFBN and RFRN) showed peaks at (1395, 874, and 713 cm^{-1}). The infrared spectrum in the region from 950-1100 cm^{-1} showed strong absorption bands for Si–O, which are formed in the silicate structure [61]. Therefore, the peaks observed at 1007 cm^{-1} is due to Si-O group that is lifted to 1034 cm^{-1} after dye adsorption. It was considered that the -SO$_3$H group is responsible for the peaks, which were appeared at 1395 and 714 cm^{-1} [62]. In deformation, the bending modes of Si-O group shifted to 1402 cm^{-1} after dye adsorption and no significant change was noticed at 714 cm^{-1} peak after adsorption. The peaks for both dyes at 874 cm^{-1} indicated the existence of CO group stretching vibration. The peaks at 2514, 2164 and 1800 cm^{-1} are associated with the bands of dolomite clay, which are connected with stretching vibration of (CO^{2-})$_3$ group that was shifted to 2507 and 1788 cm^{-1} after adsorption and the peak at 2164 cm^{-1} was disappeared in loaded clay. The peak at 3408 cm^{-1} was absent in the raw clay and it was due to -OH stretching vibrations of adsorbed water [63], which is shifted to 3617 cm^{-1} after adsorption. Therefore, the peaks appeared at 1031 cm^{-1} was due to Si-O group that is shifted to 1034 cm^{-1} after the adsorption of dye. Furthermore, the peaks appeared at 1418 and 714 cm^{-1} are correlated with -SO$_3$H group [62] and twisting and distortion modes of Si-O group

[64] were shifted to 1402 and 713 cm^{-1} after dye adsorption, respectively. The peak appeared at 874 cm^{-1} indicated the calcite CO group stretching vibration 2503, 2507 and 1800 cm^{-1} bands are associated with dolomite clay, which is due to the stretching vibration of (CO_3^{2-}) group that were shifted to 2355, 2360 and 1793 cm^{-1} after dye adsorption. The peak observed at 3734 cm^{-1} was appeared in loaded adsorbent and was absent in unloaded adsorbent that is due to the dye adsorption.

3.1.2. Thermogravimetric analysis (TGA)

Thermogravimetric analysis of the adsorbents (raw and acidified clay) is shown in **Fig. 2** for both BFBN and RFRN dyes. In raw clay for both dyes, initially, there was 20% weight loss at 175 $^{\circ}$C, which is due to interlayer water molecules and removal of adsorbed water [65]. In the second phase, 80% weight loss occurred at 175–400 $^{\circ}$C that may be due to the dehydration of the exchangeable cations which resulting in the removal of water [66]. However, the maximum weight loss occurred at 700 $^{\circ}$C. In acidified clay, the pattern of weight loss was changed, firstly 9% weight loss occurred between 35 and 75 $^{\circ}$C and then, 46% weight loss was observed at phase 2 between 75 and 350 $^{\circ}$C that is in line with reported studies [62, 67]. Then, 37% weight loss was observed in the temperatures range of 350–500 $^{\circ}$C due to the distortion of the main chain of adsorbent and dissociation of organic compounds [67]. In the end, a small weight loss of the sample was observed at 580 $^{\circ}$C in acidified clay.

3.1.3. Morphological studies

Surface morphologies of loaded and unloaded adsorbents were studied before and after adsorption of both dyes and responses thus observed are shown in **Fig. 3**. From SEM images of raw clay, it was observed that the surface of clay was smooth and fine particles committed to the external layer

(surface). However, no significant change was observed in structure with SEM analysis for acidified clay. Hence, Brunauer-Emmett-Teller (BET) analysis of only raw clay was performed and the results are presented in **Table 1** for both dyes.

3.1.4. X-ray Diffraction

XRD pattern of raw and acidified clay is presented in **Fig.4** for both dyes. Both raw and acidified clays showed similar XRD patterns, which revealed that the treatment did not disturb the structure of clay. Only the intensity of some peaks at 26.5° and 28.5° is decreased which shows decreased crystallinity of clay after acidification. The main crystalline phase including mineral clay in the XRD pattern of raw and acidified clay shows a prominent peak of Orthoclase and Albite at 23.05° and 28.5°. While the XRD pattern of non-clay phase shows 5 peaks of Quartz at 26.5°, 36.0°, 39.49°, 47.56° and 48.59° and 1 peak of Calcite at 43.21° and Dolomite at 57.51° [61, 68]. According to the results, the most commonly formed non-clay mineral in raw and acidified clay is quartz that was not eliminated even after the acidification of raw clay. This shows that quartz is resistant to acid treatment and is a stable component of the clay [69].

3.2. Effects of modification on adsorption capacity of clay

Raw, immobilized, acidified and SDS treated clays have been used to check their adsorption against BFBN and RFRN dyes. Screening experiments were performed to select the adsorbent with higher adsorption capacity. The findings (**Fig. 5**) showed that adsorption capacity of about 8.10, 8.39, 0.94 and 0.39 mg/g for BFBN and 7.86, 7.95, 0.99 and 0.85 mg/g for RFRN dye onto raw, acidified, immobilized and SDS treated clay, respectively. The maximum adsorption capacity for both BFBN and RFRN dyes were obtained by acidified clay. The order of BFBN and RFRN dyes adsorption capacities was appeared as; acidified clay > raw clay > immobilized clay > SDS

treated clay. According to Al-Essa [70], an acid that acts upon the clay increased the performance of clay by enhancing the surface area and permeability. The surface area of Jordanian bentonite clay was increased from 66.2 to 287.8 m^2/g after modification with (0.1 M) HCl. In the acid-treated clay, hydrogen ions increased on the surface of clay and electrostatic attractions established between positively charged clay and negatively charged dye anions due to which acid-treated clay showed higher adsorption capacity [71]. Because of high and comparable adsorption capacity of acidified and raw clays, both were selected for further adsorption studies.

3.3. Point of zero charge (pH$_{pzc}$) of adsorbents

A point of zero charge is the adsorption phenomena used to analyze the charge on the adsorbent surface. The negative and positive nature of the adsorbent surface is interrelated with pH$_{pzc}$. The pH above pH$_{pzc}$ results in a negatively charged adsorption surface and pH below pH$_{pzc}$ gives a positive charge to the adsorption surface [1, 2]. The responses obtained are shown in **Fig. 6**. The pH$_{pzc}$ value for both raw and acidified clay was found to be 9.0. Hence below this pH, raw and acidified clay acquires positive charge which consequences in an electrostatic attraction between anions. A negative charge appeared on the surface of raw and acidified clay (> pH$_{pzc}$) that is responsible for the adsorption of cations on negatively charged adsorbent's surface. The adsorption nature of dyes on to the adsorbent surface as a function of pH$_{pzc}$ is presented in **Fig. 7**. These findings are in agreement with previous studies that have been performed using different biocomposites [1, 2].

3.4. Effect of initial pH and dye concentration on adsorption

pH is one of the significant regulatory features of the adsorption process. The pH affects the functional groups and dye interaction with sorbents. This phenomenon was studied in the pH range

of 2–12, the dye adsorption found to be 8.10 and 8.39 mg/g for BFBN and 7.86 and 7.95 mg/g for RFRN onto raw and acidified clay respectively at pH 2 (**Fig. 8**). This was decreased for raw clay and enhanced for acidified clay when pH was increased. The extent of adsorption decreased from 8.10 to 0.09 mg/g in the case of raw clay for BFBN dye, while for RFRN dye the adsorption decreased from 7.86 to 0.24 mg/g as the pH increased to 12. However, the dye adsorption capacity of raw clay continually decreased in acidic pH and became constant between 4–7 pH range. This is due to the fact that when pH was low, the concentration of H^+ increased that compete with cations, hence the adsorption capacity decreased [25]. As the pH increased from 7 to 12, the adsorption potential of raw clay decreased and acidified clay showed higher adsorption capacity in parallel to raw clay at higher pH. The adsorption capacity of BFBN onto acidified clay decreased from 8.38 to 4.08 mg/g within the pH assortment of 2–7 and then increased to 9.85 mg/g from 8 to 12 pH. While the adsorption capacity of RFRN decreased from 7.95 to 2.93 mg/g and then increased to 10.01 mg/g within the same pH ranges. These results confirm that the treated form of adsorbent (acidified clay) showed higher dye removal versus untreated adsorbent. It may be due to acid treatment that enhances the amount of ionizable moieties available for adsorption of dyes at higher pH [25]. These findings also showed that at any pH the acidified clay has maximal dye removal as compared to the raw clay. These findings are in line with I. Chaari et al. [72] who reported that the acid activation enhanced the numbers of active sites that are responsible for dye removal at any Ph. The maximum adsorption capacity was found at pH 6 for acid-treated clay and pH 7.3 for raw clay.

The influence of changing of BFBN and RFRN dyes concentrations were examined via changing the initial concentration of dye from 10 to 100 mg/L, while keeping other parameters constant. The

findings (**Fig. 9**) revealed that the adsorption of both dyes was enhanced with an increasing concentration of dyes. As the concentration increased from 10 to 100 mg/L, the elimination of BFBN dye enhanced from 3.25 to 25.41 mg/g with acidified clay and 2.11 to 24.16 mg/g with raw respectively. The adsorption of BFBN dye enhanced from 3.36 to 18.96 mg/g with acidified clay and 3.23 to 15.90 mg/g with raw clay respectively. It is reported that the concentration of adsorbate controls the uptake of dye [1, 25]. However, after a specific concentration, the uptake capacity of raw and acidified clay slowed down that is due to the saturation of binding sites [2]. Initially, enhancement was due to the availability of active sites, which attained saturation point after a certain concentration. These findings are in line with the already reported studies that an initial concentration acts as a driving force to transfer the ions from solution to the adsorbent surface like organoclay [64], Moroccan crude clay [73] and activated bentonite clay [74] these showed a similar adsorption behaviour as a function of initial adsorbate concentration.

3.5. Effect of adsorbent concentration and contact time on adsorption

The adsorption efficiency is also dependent on the adsorbent quantity as it regulates the sorbate-adsorbent equilibrium in the sorption system. The effect of raw and acidified clay dose on both BFBN and RFRN dyes was investigated with adsorbent dose in the range of 0.05 to 0.25 g/25 mL. The adsorption capacity of 8.35 and 8.81 mg/g for BFBN dye onto raw and acidified clay was observed at 0.21 and 0.15 g adsorbent dose respectively (**Fig. 10)**. While the maximum adsorption capacity for RFRN dye for raw and acidified clay was recorded at 0.05 g adsorbent dose. Beyond this dose, the adsorption capacity of BFBN dye did not change. The reason behind this trend is that at a higher dose of adsorbent, the binding sites for dye-binding are not available due to aggregation formation of the adsorbent [2]. Furthermore, for RFRN dye, the adsorption decreased by increasing the adsorbent dose and reached to 7.70 mg/g for the adsorbent dose of 0.25 g.

Previous findings also documented similar results that the adsorbent dose has a prominent effect of adsorption. Therefore, for efficient adsorption, the optimum adsorbent dose is required. Chitosan, starch, polyaniline, polypyrrole biocomposite, polypyrrole, polyaniline, sodium alginate biocomposites, organic-inorganic (hybrid bio-nanocomposite) of cellulose and clay showed similar adsorption behaviour as a function of adsorbent dose for acid black dye, imidacloprid and Drimarine Yellow HF-3GL respectively [1, 2, 25].

Contact time is also a critical factor for the effective adsorption of any adsorbate. The efficiency of contact time on the sorption of both BFBN and RFRN dyes onto raw and acidified clay was examined over a time range of 320 min. It was noted that the uptake of BFBN and RFRN dyes onto raw and acidified clay was enhanced with contact time. The adsorption rate was fast at the initial stage, thereafter, the adsorption rate was slowed down, and equilibrium was accomplished within 80 min (**Fig. 11**). The maximum adsorption capacities observed at equilibrium were as; 8.48 and 8.92 mg/g for BFBN and 7.41 and 7.95 mg/g for RFRN onto raw and acidified clay respectively. The decline in adsorption rate was because of accessibility and binding sites on the surface of the clay, which saturated after a specific time period and later on, the adsorption process was slowed down. Zen and El-Berrichi [74] explained the role of contact time on the adsorptive removal of anionic dye (Blue Derma R67) on to bentonite clay and found that 82% absorption was achieved up to equilibrium within 40–80 min. Also, organic-inorganic (hybrid bionanocomposite) of cellulose and clay showed similar adsorption behaviour as a function of contact time for Drimarine Yellow HF-3GL [25].

3.6. Effect of temperature and thermodynamic studies

During the adsorption process, the temperature is considered as another significant feature that affects the adsorption of adsorbate, therefore, it was studied in the range of 30–50 ºC. **Fig. 12** represents the influence of temperature on adsorption of BFBN and RFRN dyes onto raw and acidified clay. The adsorption of BFBN dye was 8.74 to 8.35 mg/g with acidified clay and 8.57 to 8.26 mg/g with raw clay in the temperature range of 30 to 50 ºC. The maximum adsorption was observed at 30 ºC. While the adsorption of RFRN dye decreased from 7.70 to 7.41 mg/g for raw clay when the temperature was increased from 30 to 50 ºC. Furthermore, the adsorption capacity of acidified clay was decreased from 7.91 to 7.54 mg/g for the same temperature levels. For acidified clay, the maximum sorption capacity was obtained at 30 ºC. However, the reduction in the adsorption ability at higher temperature was due to denaturation of the active site, which further revealed that both dyes' adsorption onto both adsorbents was an exothermic process. These findings are in agreement with Toor and Jin [53], they also revealed that the adsorption capacity of clay adsorbent was decreased with temperature. Şahin et al. [61] also reported that at 30 ºC, the bentonite clay (cold plasma treated) showed a maximum adsorption ability (303 mg/g) for methylene blue dye removal and organic-inorganic (hybrid bionanocomposite) based on cellulose and clay showed similar adsorption behaviour for Drimarine Yellow HF-3GL dye as a function of temperature [25]. Furthermore, thermodynamics study was also performed and the results are presented in **Table 2** for both BFBN and RFRN dyes. The ΔH^o value for both BFBN and RFRN dyes (raw and acidified clay) was negative that revealed an exothermic nature of both dyes' adsorption. The adsorption is physical in nature if the value of ΔH^o is <40 kJ/mol. Similarly, the ΔG^0 indicates the dyes adsorption was spontaneous on both raw and modified clays since negative values were recorded for both dyes as well for adsorbents. Besides, at a solid-solution interface,

the randomness was decreased since ΔS^0 values were negative for both dyes as well as adsorbents [63]. These findings are in line with Toor and Jin [25, 53], they documented similar findings for Drimarine Yellow HF-3GL dye adsorption on to bionanocomposite based on cellulose and clay. The previous investigation also revealed that these types of dyes could be removed using composite/modified adsorbents instead of raw adsorbent, for instance, chitosan and clay composites were prepared and applied for the removal of direct Rose FRN dye as a function of composite dose, pH, initial dye concentration, contact time and temperature. The composite showed a maximum sorption capacity of 17.18 mg/g within the first 40 min of contact time. The pH_{pzc} was found to be 7.0 for chitosan and clay composites. The developed method was also applied to treat a real textile effluent for the efficient removal of dyes and efficiency was promising [75].

3.7. Adsorption kinetics

Sorption kinetics study is a critical factor to evaluate the adsorption dynamics [1]. The pseudo-first-order and pseudo-first-order kinetics models were applied on both BFBN and RFRN dyes adsorption data onto raw and acidified clay. The kinetics parameters for both models are presented in **Table 3** for both dyes as well as adsorbents. The values of R^2 for BFBN were as 0.77 for acidified and 0.68 for raw clay, similarly in the case of RFRN were 0.73 and 0.62 for raw and acidified clay respectively. The difference between the values of $q_{e,\ exp}$ (mg/g) and $q_{e,\ cal}$ (mg/g) revealed that the pseudo-first-order did not fit well to the dyes adsorption data for both adsorbents. The results are comparable with the findings of Toor and Jin, [53] which stated that the R^2 values of pseudo-first-order (0.94) were less than the pseudo-second-order (0.99) model, which indicated that the bentonite clay does not obey the pseudo-first-order model for Congo red dye removal. Similarly, the pseudo-second-order model parameters for both BFBN and RFRN dyes as well as

adsorbents are shown in **Table 3**. The R^2 values for BFBN were as 0.97 and 0.97 for raw and acidified clay, similarly in case of RFRN were 0.98 and 0.98 for raw and acidified clay respectively. This indicates that the second-order model fitted well to the adsorption data of BFBN and RFRN dyes onto raw and acidified clay. The values of $q_{e, cal}$ are much closer to the values of $q_{e, exp}$ for both dyes, which revealed the best suitability of the pseudo-second-order model. Moreover, adsorption of Congo red on bentonite-based adsorbent and Drimarine Yellow HF-3GL dye adsorption on bio-nanocomposite based on cellulose and clay showed similar adsorption behaviour [25, 53].

3.8. Adsorption isotherms

The equilibrium isotherms were evaluated for understanding the adsorption mechanism. The isotherm parameters for both dyes as well as adsorbents are presented in Table 4. The Freundlich has the highest R^2 value close to 1. The n values of Freundlich isotherm for BFBN were 0.98 and 1.45 and for RFRN were 2.03 and 1.68 in the case of raw and acidified clay respectively that revealed the fitness of this model favourably. The R^2 value for BFBN dye (0.94 for acidified and 0.96 for raw clay) revealed that Freundlich isotherm best explained the adsorption of dye onto the raw clay. While the values of correlation coefficient R^2 for RFRN dye 0.90 for acidified clay and 0.74 for raw clay showed that Freundlich isotherm was the best fit for the adsorption of dye onto acidified clay. The results are comparable to those obtained by Duman et al., [76] for adsorption of Basic Red 9 (BR9) dye by vermiculite clay. Additionally, the Freundlich model fitted well to the adsorption of diazo dye on to modified natural bentonite [53]. In the case of Langmuir isotherm, the criteria of favorability and suitability of the adsorption process is R_L value. The values of R_L were 0.001 and 0.02 for BFBN and 0.94 and 0.90 for RFRN dye in the case of raw and acidified clay respectively (**Table 4).** The values of R^2 for BFBN (0.005 and 0.87) and RFRN (0.10 and

0.13) for both clays were observed. The values of $q_{m\ exp}$ and $q_{m\ cal}$ were not in line with each other, which revealed that Langmuir isotherm is failed to explain the adsorption of BFBN and RFRN dyes. Redlich-Peterson isotherm parameters results are also shown in **Table 4.** The values of R^2 were 0.43 and 0.82 for BFBN and 0.75 and 0.69 for RFRN for raw and acidified clay respectively in Redlich-Peterson isotherm. According to the value of R^2, Redlich-Peterson isotherm is also unable to explain the dyes adsorption onto clay-based adsorbents. Hence, Freundlich isotherm is the best to explain the BFBN adsorption onto raw clay and RFRN onto acidified clay. Langmuir isotherm displayed best fitting to the experimental data of RFRN onto acidified clay and BFBN onto the raw clay.

3.9. Effect of interfering ions on adsorption of dyes

Adsorption of both dyes (BFBN and RFRN) were studied in the existence of cations including, Cu^{+2}, Ni^{+2}, Pb^{+2}, and Cd^{+2} under optimized conditions and results are depicted in **Table 5**. The influence of ions interface on the process of adsorption can be determined from the ratio of capacity of adsorption in the existence (q_{mix}) to the absence (q_o) of interfering ions. If $q_{mix}/q_o = 1$ then adsorption was not affected in the existence of other ions. If $q_{mix}/q_o < 1$ then adsorption was affected negatively in the occurrence of interfering ions and if this ratio is > 1, then sorption is enhanced in the existence of interfering ions [77]. The experiments were performed at different concentrations of cations to evaluate the influence of cations on the adsorption capacity of the clay-based adsorbents. The ratio of q_{mix}/q_o was <1 for all the cations (**Table 5**), which indicates that adsorption of BFBN and RFRN onto raw and acidified clay decreased in the presence of cations. However, at low concentrations cations exhibited no significant effect and at higher concentrations, the effect was significant. These findings are in agreement with A. Kausar et al., [78] who reported the interfering cations effect on adsorption of dyes for nano adsorbents.

3.10. Desorption studies and textile wastewater treatment

The treatment of wastewater is cost-effective if adsorbent successfully regenerated or recovered [29]. Desorption of the loaded raw and acidified clay was studied using different eluting agents like $MgSO_4$, H_2SO_4, HCl and NaOH. These loaded adsorbents were kept in contact with eluting agents and desorption was compared. The results are shown in **Fig. 13** for BFBN and RFRN dyes. The maximum desorption efficiency for BFBN dye was 84.78 and 41.05% in the case of $MgSO_4$ for raw and acidified clay respectively. In the case of RFRN dye, desorption efficiencies were 95.23 and 65.43% for raw and acidified respectively using $MgSO_4$. The higher desorption was due to low pH versus adsorption pH (basic), which enhanced desorption by weakening the adsorptive interactions between dye and adsorbent. The surface of clay was detected to be negatively charged at $pH > pH_{pzc}$. Hence, desorption was efficient at lower pH than pH_{pzc}. Furthermore, desorption efficiency of eluting agents for both raw and acidified clays decreased in the following order; $MgSO_4 > NaOH > H_2SO_4 > HCl$. The process developed is also used to treat the textile wastewater contains dyes at optimum conditions of process variables and responses obtained are shown in **Fig. 14.** At pH 2, the colour removal was 50.35 and 54.95% for raw and acidified clay respectively. Results suggested that the developed method is highly efficient and precise to treat the textile effluents. This method can be efficiently applied to remove the dyes from effluents since clays are cost-effective and eco-friendly versus other adsorbents. Under the current scenario of environmental pollution [1, 2, 11, 15, 25, 40, 51, 79-84], there is need to develop and apply eco-benign material to avoid environmental pollution [85-88], therefore, modified clay [17, 18] is excellent for the adsorption of diverse type of toxic pollutants [89, 90].

4. Conclusions

The BFBN and RFRN dyes adsorption were studied using clay-based adsorbents. The acidified clay showed higher adsorption efficiency versus raw clay. The dye adsorption was efficient at pH 2 for raw clay and at pH 12 in the case of acidified clay. Moreover, dyes initial dye concentrations, adsorbent doses and temperatures significantly affected the adsorption efficiency of the adsorbents. Foreign ions negatively affected the adsorption of both dyes in raw and acidified clays. Freundlich isotherm well fitted to the dyes adsorption data and both BFBN and RFRN dyes followed pseudo-second-order kinetics model. The dye adsorption was an exothermic, spontaneous and favourable process onto clay-based adsorbents. Furthermore, $MgSO_4$ desorbed both dyes efficiently as compared to other eluting agents including; $NaOH$, H_2SO_4 and HCl. Therefore, it is concluded that acidified clay can be used efficiently for the removal of synthetic dyes from real textile effluent since it is effective, eco-friendly and reasonable adsorbent for wastewater treatment.

References

[1] F. Ishtiaq, H.N. Bhatti, A. Khan, M. Iqbal, A. Kausar, Polypyrole, polyaniline and sodium alginate biocomposites and adsorption-desorption efficiency for imidacloprid insecticide, Int. J. Biol. Macromol. 147 (2020) 217-232.

[2] S. Noreen, H.N. Bhatti, M. Iqbal, F. Hussain, F.M. Sarim, Chitosan, starch, polyaniline and polypyrrole biocomposite with sugarcane bagasse for the efficient removal of Acid Black dye, Int. J. Biol. Macromol. 147 (2020) 439-452.

[3] M. Bilal, M. Asgher, M. Iqbal, H. Hu, X. Zhang, Chitosan beads immobilized manganese peroxidase catalytic potential for detoxification and decolorization of textile effluent, Int. J. Biol. Macromol. 89 (2016) 181-189.

[4] D.N. Iqbal, M. Tariq, S.M. Khan, N. Gull, S. Sagar Iqbal, A. Aziz, A. Nazir, M. Iqbal, Synthesis and characterization of chitosan and guar gum based ternary blends with polyvinyl alcohol, Int. J. Biol. Macromol. 143 (2020) 546-554.

[5] N. Tahir, H.N. Bhatti, M. Iqbal, S. Noreen, Biopolymers composites with peanut hull waste biomass and application for Crystal Violet adsorption, Int. J. Biol. Macromol. 94 (2016) 210-220.

[6] T. Benhalima, H. Ferfera-Harrar, Eco-friendly porous carboxymethyl cellulose/dextran sulfate composite beads as reusable and efficient adsorbents of cationic dye methylene blue, Int. J. Biol. Macromol. 132 (2019) 126-141.

[7] V. Javanbakht, R. Shafiei, Preparation and performance of alginate/basil seed mucilage biocomposite for removal of eriochrome black T dye from aqueous solution, Int. J. Biol. Macromol. (2019). https://doi.org/10.1016/j.ijbiomac.2019.10.185

[8] L. Li, J. Iqbal, Y. Zhu, P. Zhang, W. Chen, A. Bhatnagar, Y. Du, Chitosan/Ag-hydroxyapatite nanocomposite beads as a potential adsorbent for the efficient removal of toxic aquatic pollutants, Int. J. Biol. Macromol. 120 (2018) 1752-1759.

[9] T. Lou, X. Yan, X. Wang, Chitosan coated polyacrylonitrile nanofibrous mat for dye adsorption, Int. J. Biol. Macromol. 135 (2019) 919-925.

[10] A.M. Alkherraz, A.K. Ali, K.M. Elsherif, Removal of Pb(II), Zn(II), Cu(II) and Cd(II) from aqueous solutions by adsorption onto olive branches activated carbon: Equilibrium and thermodynamic studies, Chem. Int. 6(1) (2020) 11-20.

[11] N.E. Ibisi, C.A. Asoluka, Use of agro-waste (*Musa paradisiaca* peels) as a sustainable biosorbent for toxic metal ions removal from contaminated water, Chem. Int. 4(1) (2018) 52-59.

[12] M. Fazal-ur-Rehman, Current scenario and future prospects of activated carbon preparation from agro-industrial wastes: A review, Chem. Int. 4(2) (2018) 109-119.

[13] O. Chidi, R. Kelvin, Surface interaction of sweet potato peels (*Ipomoea batata*) with Cd(II) and Pb(II) ions in aqueous medium, Chem. Int. 4(4) (2018) 221-229.

[14] K. Legrouri, E. Khouya, H. Hannache, M. El Hartti, M. Ezzine, R. Naslain, Activated carbon from molasses efficiency for Cr (VI), Pb (II) and Cu (II) adsorption: A mechanistic study, Chem. Int. 3(3) (2017) 301-310.

[15] A.M. Alasadi, F.I. Khaili, A.M. Awwad, Adsorption of Cu(II), Ni(II) and Zn(II) ions by nano kaolinite: Thermodynamics and kinetics studies, Chem. Int. 5(4) (2019) 258-268.

[16] E.C. Jennifer, O.P. Ifedi, Modification of natural bentonite clay using cetyl trimetyl-ammonium bromide and its adsorption capability on some petrochemical wastes, Chem. Int. 5(4) (2019) 269-273.

[17] M. Alaqarbeh, M. Shammout, A. Awwad, Nano platelets kaolinite for the adsorption of toxic metal ions in the environment, Chem. Int. 6 (2020) 49-55.

[18] A.M. Awwad, M.W. Amer, M.M. Al-Aqarbeh, TiO_2-kaolinite nanocomposite prepared from the Jordanian Kaolin clay: Adsorption and thermodynamic of Pb(II) and Cd(II) ions in aqueous solution, Chem. Int. 6(4) (2020) 168-178.

[19] A. García, M. Culebras, M.N. Collins, J.J. Leahy, Stability and rheological study of sodium carboxymethyl cellulose and alginate suspensions as binders for lithium ion batteries, J. Appl. Polym. Sci. 135(17) (2018) 46217.

[20] A. Ayach, S. Fakhi, Z. Faiz, A. Bouih, O. Ait malek, A. Benkdad, M. Benmansour, A. Laissaoui, M. Adjour, Y. Elbatal, I. Vioque, G. Manjon, Adsorption of methylene blue on bituminous schists from Tarfaya-Boujdour, Chem. Int. 3(4) (2017) 442-451.

[21] P. Sharma, D.J. Borah, P. Das, M.R. Das, Cationic and anionic dye removal from aqueous solution using montmorillonite clay: evaluation of adsorption parameters and mechanism, Desalin. Water Treat. 57(18) (2016) 8372-8388.

[22] T. Taher, D. Rohendi, R. Mohadi, A. Lesbani, Congo red dye removal from aqueous solution by acid-activated bentonite from sarolangun: kinetic, equilibrium, and thermodynamic studies, Arab J. Basic Appl. Sci. 26(1) (2019) 125-136.

[23] A. Adewuyi, R.A. Oderinde, Chemically modified vermiculite clay: a means to remove emerging contaminant from polluted water system in developing nation, Polym. Bull. 76(10) (2019) 4967-4989.

[24] D. Ozdes, C. Duran, H.B. Senturk, H. Avan, B. Bicer, Kinetics, thermodynamics, and equilibrium evaluation of adsorptive removal of methylene blue onto natural illitic clay mineral, Desalin. Water Treat. 52(1-3) (2014) 208-218.

[25] A. Kausar, R. Shahzad, J. Iqbal, N. Muhammad, S.M. Ibrahim, M. Iqbal, Development of new organic-inorganic, hybrid bionanocomposite from cellulose and clay for enhanced removal of Drimarine Yellow HF-3GL dye, Int. J. Biol. Macromol. 149 (2020) 1059-1071.

[26] A. Kausar, M. Iqbal, A. Javed, K. Aftab, Z.-i.-H. Nazli, H.N. Bhatti, S. Nouren, Dyes adsorption using clay and modified clay: A review, J. Mol. Liq. 256 (2018) 395-407.

[27] D. Chen, Q. Zhu, F. Zhou, X. Deng, F. Li, Synthesis and photocatalytic performances of the TiO_2 pillared montmorillonite, J. Hazard. Mater. 235 (2012) 186-193.

[28] E. Eren, Removal of basic dye by modified Unye bentonite, Turkey, J. Hazard. Mater. 162(2-3) (2009) 1355-1363.

[29] T. Anirudhan, P. Suchithra, Adsorption characteristics of humic acid-immobilized amine modified polyacrylamide/bentonite composite for cationic dyesin aqueous solutions, J. Environ. Sci. 21(7) (2009) 884-891.

[30] H.A. Shindy, M.A. El-Maghraby, M.M. Goma, N.A. Harb, Dicarbocyanine and tricarbocyanine dyes: Novel synthetic approaches, photosensitization evaluation and antimicrobial screening, Chem. Int. 6(1) (2020) 30-41.

[31] H.A. Shindy, M.A. El-Maghraby, M.M. Goma, N.A. Harb, Heptamethine and nonamethine cyanine dyes: novel synthetic strategy, electronic transitions, solvatochromic and halochromic evaluation, Chem. Int. 6(4) (2020) 187-199.

[32] H.A. Shindy, Basics in colors, dyes and pigments chemistry: A review, Chem. Int. 2(1) (2016) 29-36.

[33] H.A. Shindy, Problems and solutions in colors, dyes and pigments chemistry: A Review, Chem. Int. 3(2) (2017) 97-105.

[34] U.H. Siddiqua, S. Ali, M. Iqbal, T. Hussain, Relationship between structures and dyeing properties of reactive dyes for cotton dyeing, J. Mol. Liq. 241 (2017) 839-844.

[35] H.N. Bhatti, A. Jabeen, M. Iqbal, S. Noreen, Z. Naseem, Adsorptive behavior of rice bran-based composites for malachite green dye: Isotherm, kinetic and thermodynamic studies, J. Mol. Liq. 237 (2017) 322-333.

[36] L. Bulgariu, L.B. Escudero, O.S. Bello, M. Iqbal, J. Nisar, K.A. Adegoke, F. Alakhras, M. Kornaros, I. Anastopoulos, The utilization of leaf-based adsorbents for dyes removal: A review, J. Mol. Liq. 276 (2019) 728-747.

[37] M.Z. Ahmad, I.A. Bhatti, K. Qureshi, N. Ahmad, J. Nisar, M. Zuber, A. Ashar, H. Rizvi, M.I. Khan, M. Iqbal, Graphene oxide supported $Fe_2(MoO_4)_3$ nano rods assembled round-ball fabrication via hydrothermal route and photocatalytic degradation of nonsteroidal anti-inflammatory drug, J. Mol. Liq. (2019) 112343.

[38] M. Abbas, M. Adil, S. Ehtisham-ul-Haque, B. Munir, M. Yameen, A. Ghaffar, G.A. Shar, M. Asif Tahir, M. Iqbal, Vibrio fischeri bioluminescence inhibition assay for ecotoxicity assessment: A review, Sci. Total Environ. 626 (2018) 1295-1309.

[39] M. Iqbal, *Vicia faba* bioassay for environmental toxicity monitoring: A review, Chemosphere 144 (2016) 785-802.

[40] M. Iqbal, M. Abbas, A. Nazir, A.Z. Qamar, Bioassays based on higher plants as excellent dosimeters for ecotoxicity monitoring: A review, Chem. Int. 5(1) (2019) 1-80.

[41] M. Arshad, A. Qayyum, G. Abbas, R. Haider, M. Iqbal, A. Nazir, Influence of different solvents on portrayal and photocatalytic activity of tin-doped zinc oxide nanoparticles, J. Mol. Liq. 260 (2018) 272-278.

[42] A. Kausar, M. Iqbal, A. Javed, K. Aftab, H.N. Bhatti, S. Nouren, Dyes adsorption using clay and modified clay: a review, J. Mol. Liq. 256 (2018) 395-407.

[43] A. Kausar, G. MacKinnon, A. Alharthi, J. Hargreaves, H.N. Bhatti, M. Iqbal, A green approach for the removal of Sr(II) from aqueous media: Kinetics, isotherms and thermodynamic studies, J. Mol. Liq. 257 (2018) 164-172.

[44] K. Qureshi, M.Z. Ahmad, I.A. Bhatti, M. Zahid, J. Nisar, M. Iqbal, Graphene oxide decorated $ZnWO_4$ architecture synthesis, characterization and photocatalytic activity evaluation, J. Mol. Liq. 285 (2019) 778-789.

[45] A. Babarinde, G.O. Onyiaocha, Equilibrium sorption of divalent metal ions onto groundnut (*Arachis hypogaea*) shell: kinetics, isotherm and thermodynamics, Chem. Int. 2(3) (2016) 37-46.

[46] N. Benabdallah, D. Harrache, A. Mir, M. De La Guardia, F. Benhachem, Bioaccumulation of trace metals by red alga Corallina elongata in the coast of Beni Saf, west coast, Algeria, Chem. Int. 3(3) (2017) 220-231.

[47] K.B. Daij, S. Bellebia, Z. Bengharez, Comparative experimental study on the COD removal in aqueous solution of pesticides by the electrocoagulation process using monopolar iron electrodes, Chem. Int. 3(4) (2017) 420-427.

[48] K. Djehaf, A.Z. Bouyakoub, R. Ouhib, H. Benmansour, A. Bentouaf, A. Mahdad, N. Moulay, D. Bensaid, M. Ameri, Textile wastewater in Tlemcen (Western Algeria): Impact, treatment by combined process, Chem. Int. 3(4) (2017) 414-419.

[49] M.A. Jamal, M. Muneer, M. Iqbal, Photo-degradation of monoazo dye blue 13 using advanced oxidation process, Chem. Int. 1(1) (2015) 12-16.

[50] F. Minas, B.S. Chandravanshi, S. Leta, Chemical precipitation method for chromium removal and its recovery from tannery wastewater in Ethiopia, Chem. Int. 3(4) (2017) 392-405.

[51] N. Oussama, H. Bouabdesselam, N. Ghaffour, L. Abdelkader, Characterization of seawater reverse osmosis fouled membranes from large scale commercial desalination plant, Chem. Int. 5(2) (2019) 158-167.

[52] K. Qureshi, M. Ahmad, I. Bhatti, M. Iqbal, A. Khan, Cytotoxicity reduction of wastewater treated by advanced oxidation process, Chem. Int. 1(53) (2015) e59.

[53] M. Toor, B. Jin, Adsorption characteristics, isotherm, kinetics, and diffusion of modified natural bentonite for removing diazo dye, Chem. Eng. J. 187 (2012) 79-88.

[54] G. Bayramoğlu, M.Y. Arıca, Biosorption of benzidine based textile dyes Direct Blue 1 and Direct Red 128 using native and heat-treated biomass of Trametes versicolor, J. Hazard. Mater. 143(1-2) (2007) 135-143.

[55] H. Fan, L. Zhou, X. Jiang, Q. Huang, W. Lang, Adsorption of Cu^{2+} and methylene blue on dodecyl sulfobetaine surfactant-modified montmorillonite, Appl. Clay Sci. 95 (2014) 150-158.

[56] Y. Ho, G. McKay, Comparative sorption kinetic studies of dye and aromatic compounds onto fly ash, J. Environ. Sci. Health A 34(5) (1999) 1179-1204.

[57] Y.-S. Ho, G. McKay, Pseudo-second order model for sorption processes, Proces. Biochem. 34(5) (1999) 451-465.

[58] H. Freundlich, Over the adsorption in solution, J. Phys. Chem. 57(385471) (1906) 1100-1107.

[59] I. Langmuir, The adsorption of gases on plane surfaces of glass, mica and platinum, J. Am. Chem. Soc. 40(9) (1918) 1361-1403.

[60] C. Obi, M.U. Ibezim-Ezeani, E.J. Nwagbo, Production of biodiesel using novel *C. lepodita* oil in the presence of heterogeneous solid catalyst, Chem. Int. 6(2) (2020) 91-97.

[61] Ö. Şahin, M. Kaya, C. Saka, Plasma-surface modification on bentonite clay to improve the performance of adsorption of methylene blue, Appl. Clay Sci. 116 (2015) 46-53.

[62] D. Moraes, R. Angélica, C. Costa, G. Rocha Filho, J. Zamian, Bentonite functionalized with propyl sulfonic acid groups used as catalyst in esterification reactions, Appl. Clay Sci. 51(3) (2011) 209-213.

[63] A. Öztürk, E. Malkoc, Adsorptive potential of cationic Basic Yellow 2 (BY2) dye onto natural untreated clay (NUC) from aqueous phase: mass transfer analysis, kinetic and equilibrium profile, Appl. Surf. Sci. 299 (2014) 105-115.

[64] T. Anirudhan, M. Ramachandran, Adsorptive removal of basic dyes from aqueous solutions by surfactant modified bentonite clay (organoclay): kinetic and competitive adsorption isotherm, Proces. Saf. Environ. Protect. 95 (2015) 215-225.

[65] F.G. Alabarse, R.V. Conceição, N.M. Balzaretti, F. Schenato, A.M. Xavier, *In-situ* FTIR analyses of bentonite under high-pressure, Appl. Clay Sci. 51(1-2) (2011) 202-208.

[66] C.-H. Zhou, D. Zhang, D.-S. Tong, L.-M. Wu, W.-H. Yu, S. Ismadji, like composites of cellulose acetate–organo-montmorillonite for removal of hazardous anionic dye in water, Chem. Eng. J. 209 (2012) 223-234.

[67] A. Vanamudan, P. Pamidimukkala, Chitosan, nanoclay and chitosan–nanoclay composite as adsorbents for Rhodamine-6G and the resulting optical properties, Int. J. Biol. Macromol. 74 (2015) 127-135.

[68] M. Elhadj, A. Samira, T. Mohamed, F. Djawad, A. Asma, N. Djamel, Removal of Basic Red 46 dye from aqueous solution by adsorption and photocatalysis: equilibrium, isotherms, kinetics, and thermodynamic studies, Separat. Sci. Technol. (2019) 1-19.

[69] A. Amari, H. Gannouni, M. Khan, M. Almesfer, A. Elkhaleefa, A. Gannouni, Effect of structure and chemical activation on the adsorption properties of green clay minerals for the removal of cationic dye, Appl. Sci. 8(11) (2018) 2302.

[70] K. Al-Essa, Activation of Jordanian bentonite by hydrochloric acid and its potential for olive mill wastewater enhanced treatment, J. Chem. 2018 (2018) 1-9.

[71] B. Sarkar, R. Rusmin, U.C. Ugochukwu, R. Mukhopadhyay, K.M. Manjaiah, Modified clay minerals for environmental applications, Modified Clay and Zeolite Nanocomposite Materials, Elsevier (2019) pp. 113-127.

[72] I. Chaari, M. Feki, M. Medhioub, E. Fakhfakh, F. Jamoussi, Adsorption of a textile dye Indanthrene Blue RS (CI Vat Blue 4) from aqueous solutions onto smectite-rich clayey rock, J. Hazard. Mater. 172(2-3) (2009) 1623-1628.

[73] A.B. Karim, B. Mounir, M. Hachkar, M. Bakasse, A. Yaacoubi, Removal of Basic Red 46 dye from aqueous solution by adsorption onto Moroccan clay, J. Hazard. Mater. 168(1) (2009) 304-309.

[74] S. Zen, F.Z. El Berrichi, Adsorption of tannery anionic dyes by modified kaolin from aqueous solution, Desalin. Water Treat. 57(13) (2016) 6024-6032.

[75] A. Kausar, K. Naeem, T. Hussain, Z.-i.-H. Nazli, H.N. Bhatti, F. Jubeen, A. Nazir, M. Iqbal, Preparation and characterization of chitosan/clay composite for direct Rose FRN dye removal from aqueous media: comparison of linear and non-linear regression methods, J. Mater. Res. Technol. 8(1) (2019) 1161-1174.

[76] O. Duman, S. Tunç, T.G. Polat, Determination of adsorptive properties of expanded vermiculite for the removal of CI Basic Red 9 from aqueous solution: kinetic, isotherm and thermodynamic studies, Appl. Clay Sci. 109 (2015) 22-32.

[77] F.V. Pereira, L.V.A. Gurgel, L.F. Gil, Removal of Zn^{2+} from aqueous single metal solutions and electroplating wastewater with wood sawdust and sugarcane bagasse modified with EDTA dianhydride (EDTAD), J. Hazard. Mater. 176(1-3) (2010) 856-863.

[78] A. Kausar, K. Naeem, T. Hussain, H.N. Bhatti, F. Jubeen, A. Nazir, M. Iqbal, Preparation and characterization of chitosan/clay composite for direct Rose FRN dye removal from aqueous media: comparison of linear and non-linear regression methods, J. Mater. Res. Technol. 8(1) (2019) 1161-1174.

[79] V.O. Izionworu, C.P. Ukpaka, E.E. Oguzie, Green and eco-benign corrosion inhibition agents: Alternatives and options to chemical based toxic corrosion inhibitors, Chem. Int. 6(4) (2020) 232-259.

[80] I.A. Adetutu, G.N. Iwuoha, H. Michael Jnr, Carcinogenicity of dioxin-like polychlorinated biphenyls in transformer soil in vicinity of University of Port Harcourt, Choba, Nigeria, Chem. Int. 6(3) (2020) 144-150.

[81] G.N. Iwuoha, A. Akinseye, Toxicological symptoms and leachates quality in Elelenwo, Rivers State, Nigeria, Chem. Int. 5(3) (2019) 198-205.

[82] M. Sasmaz, E. Öbek, A. Sasmaz, Bioaccumulation of cadmium and thallium in Pb-Zn tailing waste water by Lemna minor and Lemna gibba, Appl. Geochem. 100 (2019) 287-292.

[83] M. Palutoglu, B. Akgul, V. Suyarko, M. Yakovenko, N. Kryuchenko, A. Sasmaz, Phytoremediation of cadmium by native plants grown on mining soil, Bull. Environ. Contam. Toxicol. 100(2) (2018) 293-297.

[84] F. Deeba, N. Abbas, M.T. Butt, M. Irfan, Ground water quality of selected areas of Punjab and Sind Provinces, Pakistan: Chemical and microbiological aspects, Chem. Int. 5(4) (2019) 241-246.

[85] A.M. Awwad, N.M. Salem, M.M. Aqarbeh, F.M. Abdulaziz, Green synthesis, characterization of silver sulfide nanoparticles and antibacterial activity evaluation, Chem. Int. 6(1) (2020) 42-48.

[86] A.M. Awwad, M.W. Amer, N.M. Salem, A.O. Abdeen, Green synthesis of zinc oxide nanoparticles (ZnO-NPs) using Ailanthus altissima fruit extracts and antibacterial activity, Chem. Int. 6(3) (2020) 151-159.

[87] A.M. Awwad, M.W. Amer, Biosynthesis of copper oxide nanoparticles using Ailanthus altissima leaf extract and antibacterial activity, Chem. Int. 6(4) (2020) 210-217.

[88] L.S. Al Banna, N.M. Salem, G.A. Jaleel, A.M. Awwad, Green synthesis of sulfur nanoparticles using Rosmarinus officinalis leaves extract and nematicidal activity against Meloidogyne javanica, Chem. Int. 6(3) (2020) 137-143.

[89] H.N. Bhatti, Z. Mahmood, A. Kausar, S.M. Yakout, O.H. Shair, M. Iqbal, Biocomposites of polypyrrole, polyaniline and sodium alginate with cellulosic biomass: Adsorption-desorption, kinetics and thermodynamic studies for the removal of 2,4-dichlorophenol, Int. J. Biol. Macromol. 153 (2020) 146-157.

[90] H.N. Bhatti, Y. Safa, S.M. Yakout, O.H. Shair, M. Iqbal, A. Nazir, Efficient removal of dyes using carboxymethyl cellulose/alginate/polyvinyl alcohol/rice husk composite: Adsorption/desorption, kinetics and recycling studies, Int. J. Biol. Macromol. 150 (2020) 861-870.

List of Tables

Table 1. Surface analysis of raw clay used for composite preparation.

Parameters	Values
Surface area (m^2/g)	8.41
Pore volume (cm^3/g)	0.04
Pore size (Å)	19.92
Nanoparticle size (Å)	7,129.83

Table 2. Thermodynamic parameters for BFBN and RFRN dyes adsorption onto raw and modified clay as a function of temperature.

Temperature ºC	Thermodynamic parameters for BFBN dye						Thermodynamic parameters for BFBN dye					
	Raw clay			Modified clay			Raw clay			Modified clay		
	ΔG^o	ΔH^o	ΔS^o	ΔG^o	ΔH^o	ΔS^o	ΔG^o	ΔH^o	ΔS^o	ΔG^o	ΔH^o	ΔS^o
30	-330.72			-354.29			-79.37			102.96		
35	-367.14			-390.97			-77.91			-101.08		
40	-403.56	-112.19	7.28	-427.65	-134.21	7.33	-76.45	-88.13	-0.29	-99.20	-114.24	-0.37
45	-439.98			-464.33			-74.99			-97.32		
50	-476.41			-501.01			-73.52			-95.44		

Note: ΔG^o (kJ/mol), ΔH^o (kJ/mol), ΔS^o (J/ mol K).

Table 3. Evaluation of kinetics parameters for BFBN and RFRN dyes adsorption onto raw and modified clay.

Kinetic Parameters	BFBN dye		RFRN dye	
	Raw clay	Modified clay	Raw clay	Modified clay
Pseudo-first order				
K_1 (L/min)	0.01	0.00	0.01	0.01
$q_{e,}$ cal (mg/g)	4.97	5.54	4.51	4.30
$q_{e,}$ exp (mg/g)	8.48	8.92	7.41	7.90
R^2	0.68	0.76	0.73	0.62
Pseudo-second order				
K_2 (g/mg min)	0.00	0.00	0.003	0.004
$q_{e,}$ cal (mg/g)	9.54	9.68	8.15	8.25
$q_{e,}$ exp (mg/g)	8.48	8.92	8.49	8.92
R^2	0.97	0.97	0.98	0.98

Table 4. Isotherms parameters for adsorption of BFBN and RFRN dyes onto raw and modified clay following the linear regression method.

Isothermal Parameters	BFBN dye		RFRN dye	
	Raw clay	Modified clay	Raw clay	Modified clay
Langmuir				
$q_{m,}$ cal (mg/g)	714.28	4.11	19.76	25.71
$q_{m,}$ exp (mg/g)	25.05	25.41	15.90	18.97
K_L (L/mg)	8.95	0.34	0.13	0.09
R_L	0.00	0.02	0.10	0.14
R^2	0.00	0.87	0.94	0.90
Freundlich				
K_F (mg/g (mg/L)$^{-1/nF}$	0.59	1.97	1.12	2.75
n	0.97	1.44	2.03	1.68
$q_{m,}$ cal (mg/g)	26.90	30.76	15.85	21.98
$q_{m,}$ exp (mg/g)	25.05	25.41	15.90	18.97
R^2	0.95	0.93	0.74	0.90
Redlich Peterson				
A (L/mg)	2.80	1.50	6.00	5.00
B (dm^3/mg)^g	4.02	0.03	1.30	1.10
g	0.14	1.00	0.59	0.51
R^2	0.43	0.82	0.75	0.69

Table 5. Comparison of the effect of different interfering cations on BFBN and RFRN dye adsorption onto raw and modified clay.

Cations	BFBN dye						RFRN dye					
	Raw clay			Modified clay			Raw clay			Modified clay		
	5 mg/L	10 mg/L	15 mg/L	5 mg/L	10 mg/L	15 mg/L	5 mg/L	10 mg/L	15 mg/L	5 mg/L	10 mg/L	15 mg/L
Ni^{+2}	0.74	0.78	0.82	0.98	0.99	0.94	0.20	0.56	0.66	0.30	0.54	0.90
Cd^{+2}	0.95	0.93	0.92	0.76	0.79	0.74	0.47	0.45	0.43	0.36	0.49	0.85
Cu^{+2}	0.38	0.47	0.49	0.45	0.47	0.46	0.05	0.05	0.07	0.10	0.14	0.21
Pb^{+2}	0.95	0.94	0.93	0.98	0.99	0.92	0.35	0.67	0.69	0.77	0.78	0.88

List of Figures
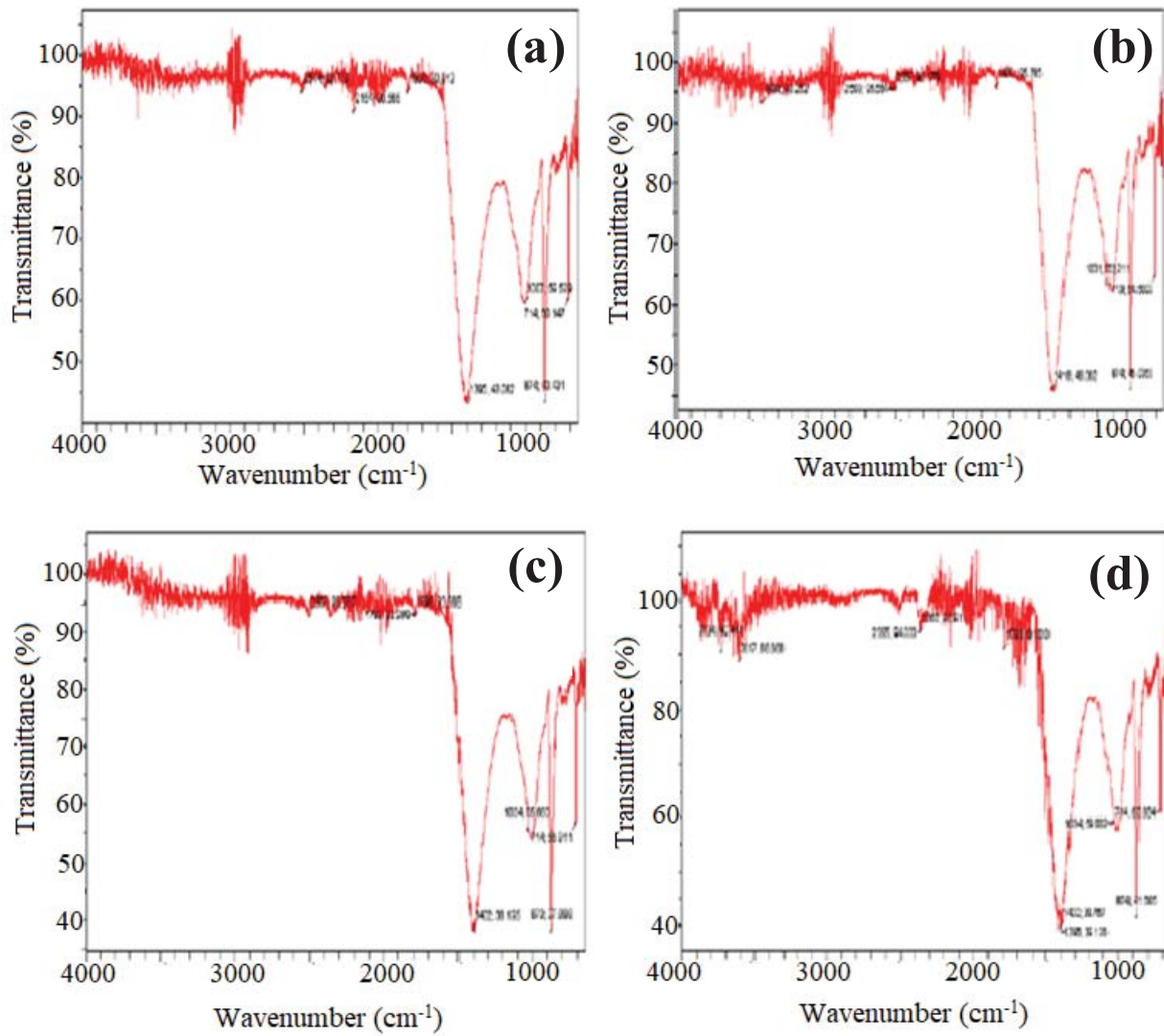
Fig. 1: FTIR spectra of clays; (a) unloaded raw clay, (b) unloaded acidified clay, (c) raw clay loaded with BFBN and (d) modified clay loaded with BFBN dye.
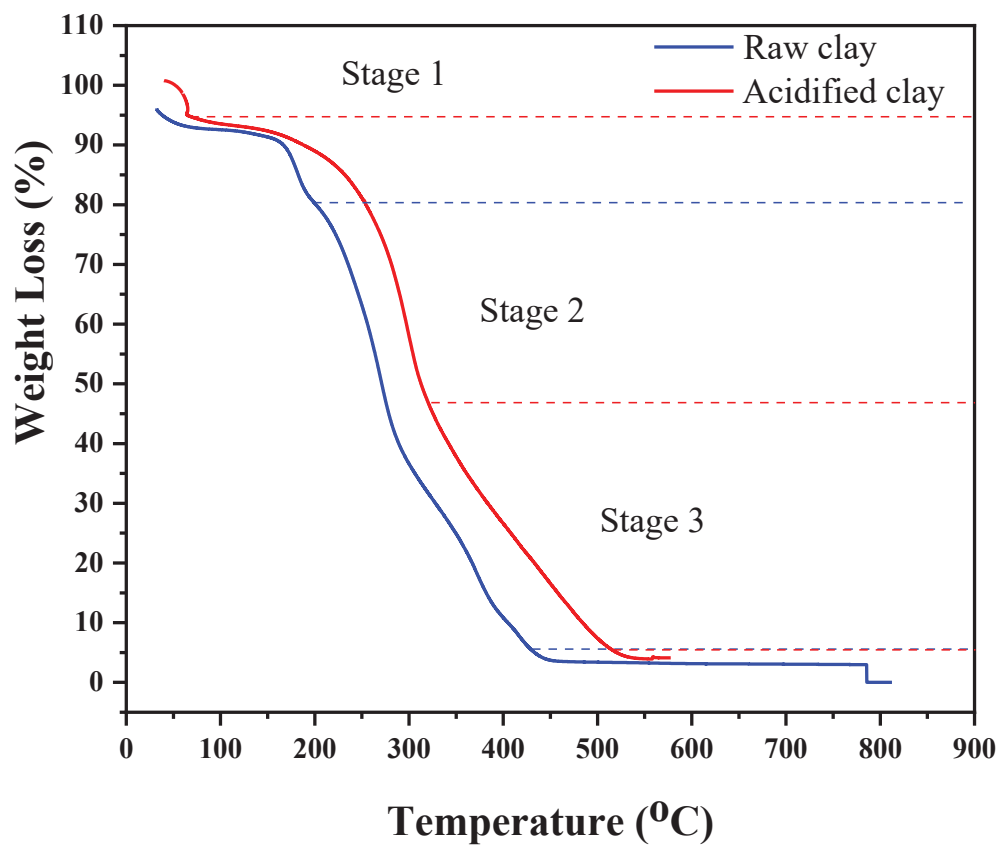
Fig. 2: Thermogravimetric analysis (TGA) of raw and modified clay adsorbents.
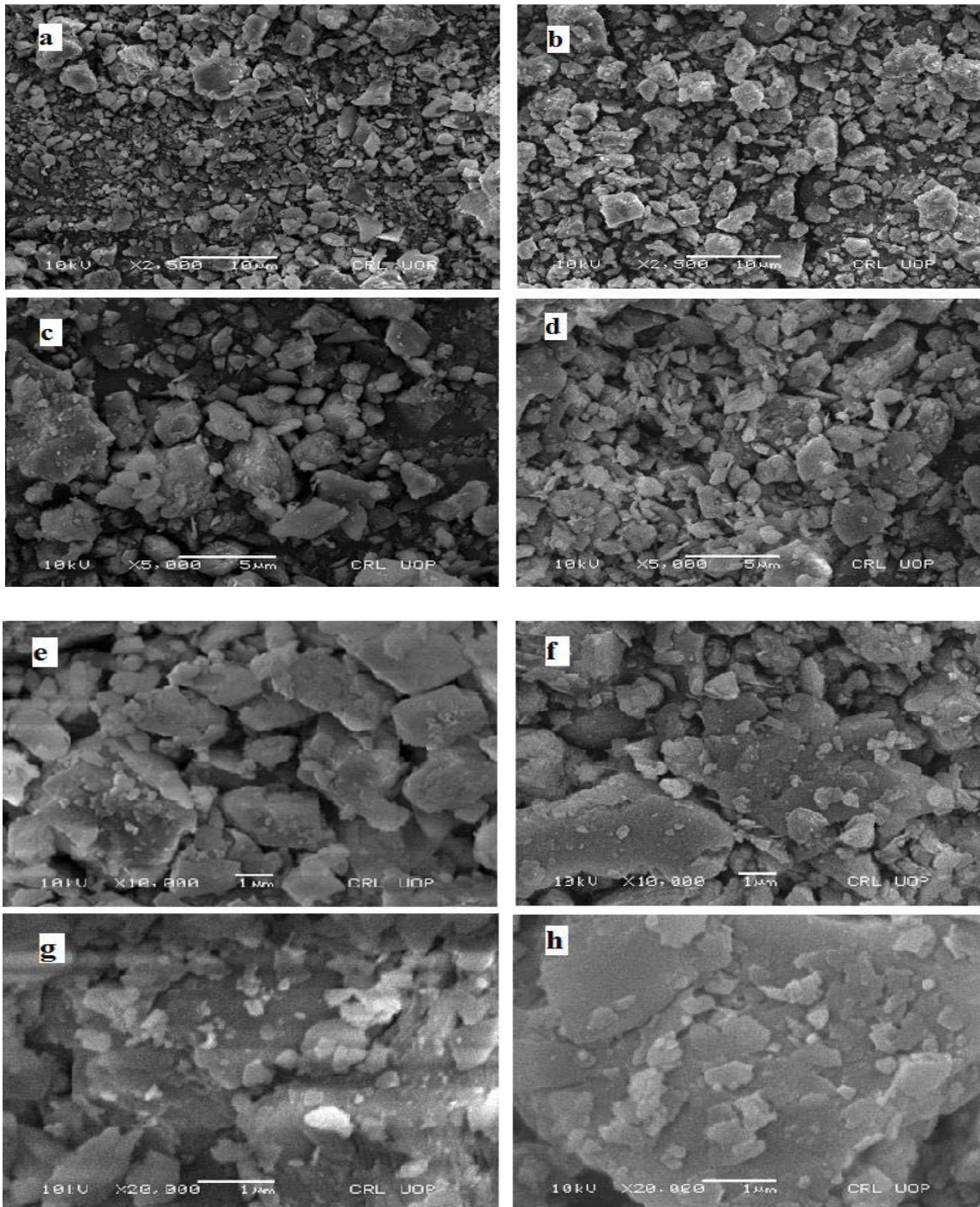
Fig. 3: SEM analysis of adsorbents; raw (a, c, e, g) and modifired clay (b, d, f, h).
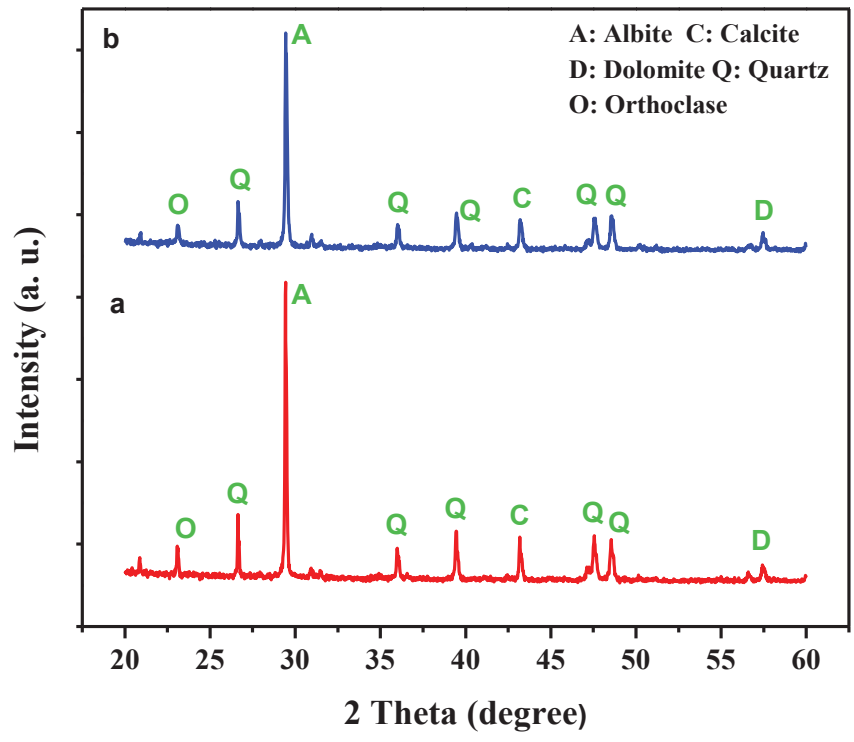
Fig. 4: The X-ray diffraction analysis of clays; (a) raw and (b) modified clay.
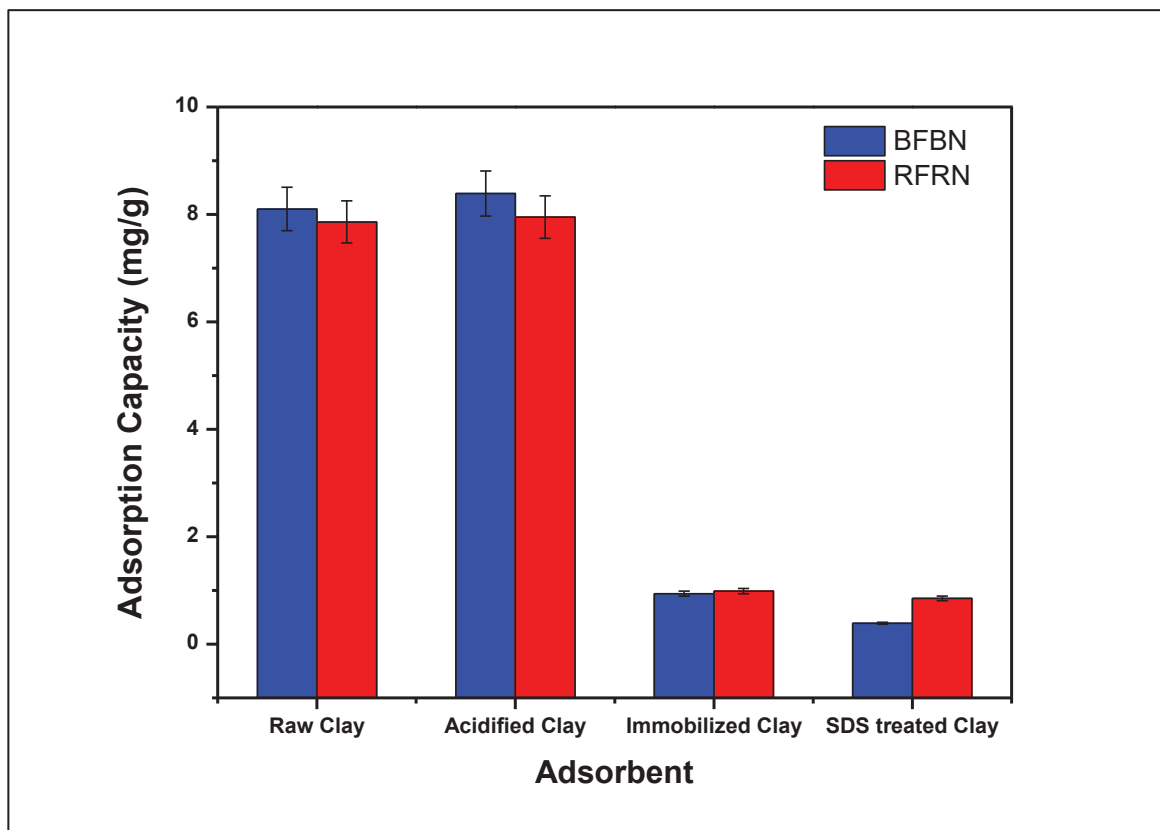
Fig. 5: Adsorption capacity of different raw and modified clays for the removal of BFBN and RFRN dyes.
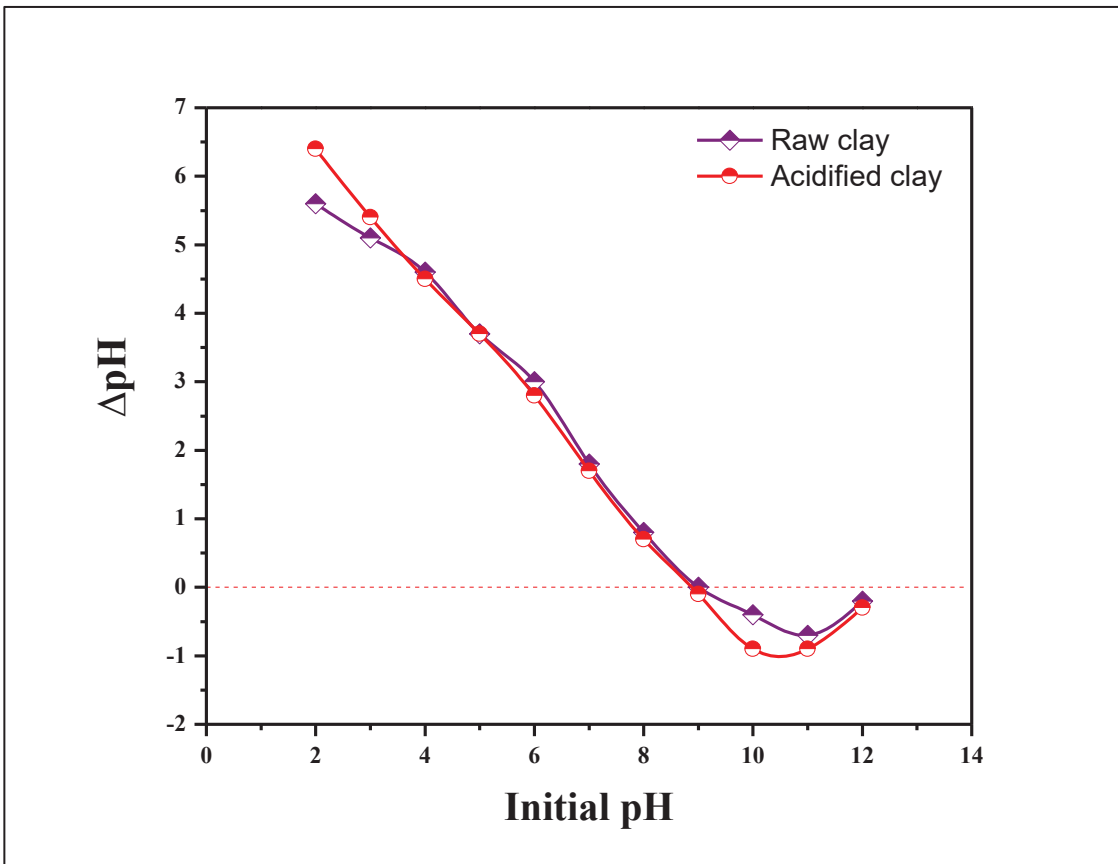
Fig. 6: Point of zero charge of raw clay and modified clay.
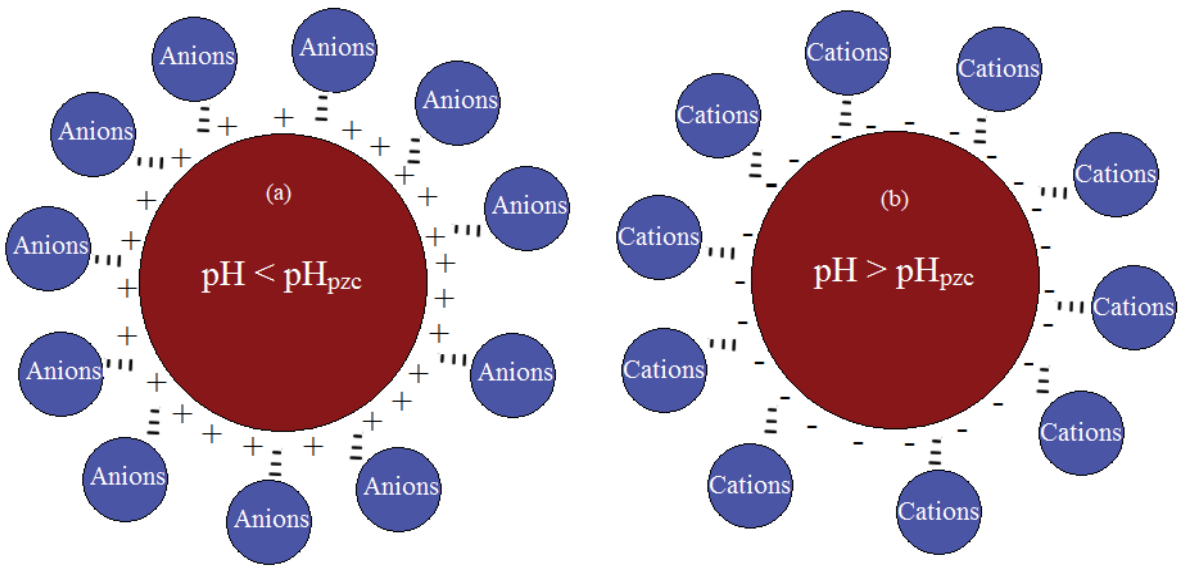
Fig. 7. Adsorption mechanism of dyes as a function of point of zero charge (pH_{pzc}) onto adsorbents; (a) When $pH < pH_{pzc}$ and (b) When $pH > pH_{pzc}$.
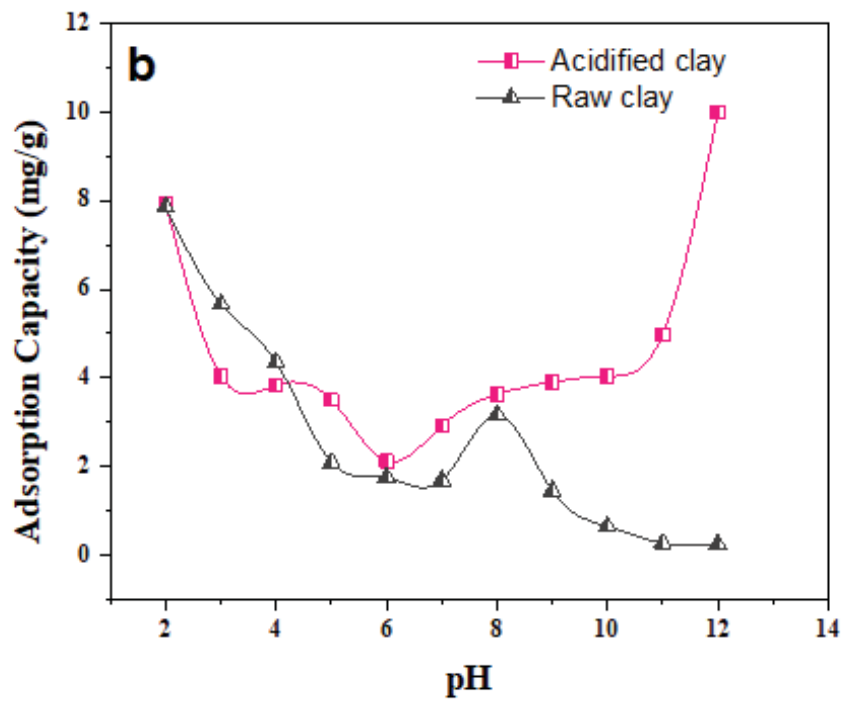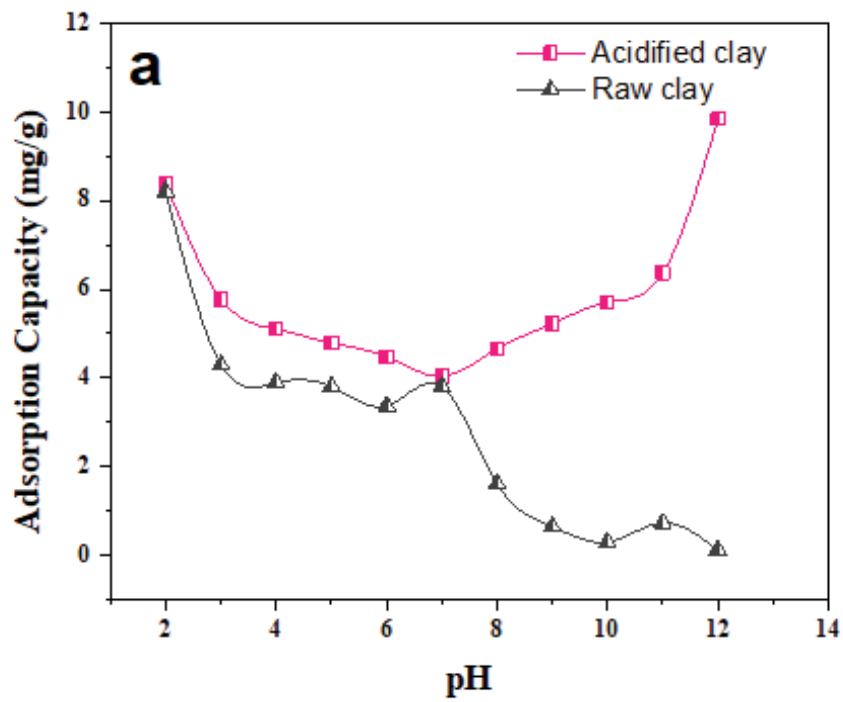
Fig. 8. Effect of pH on the removal of dyes onto raw and modified clay; (a) BFBN dye and (b) RFRN dye.
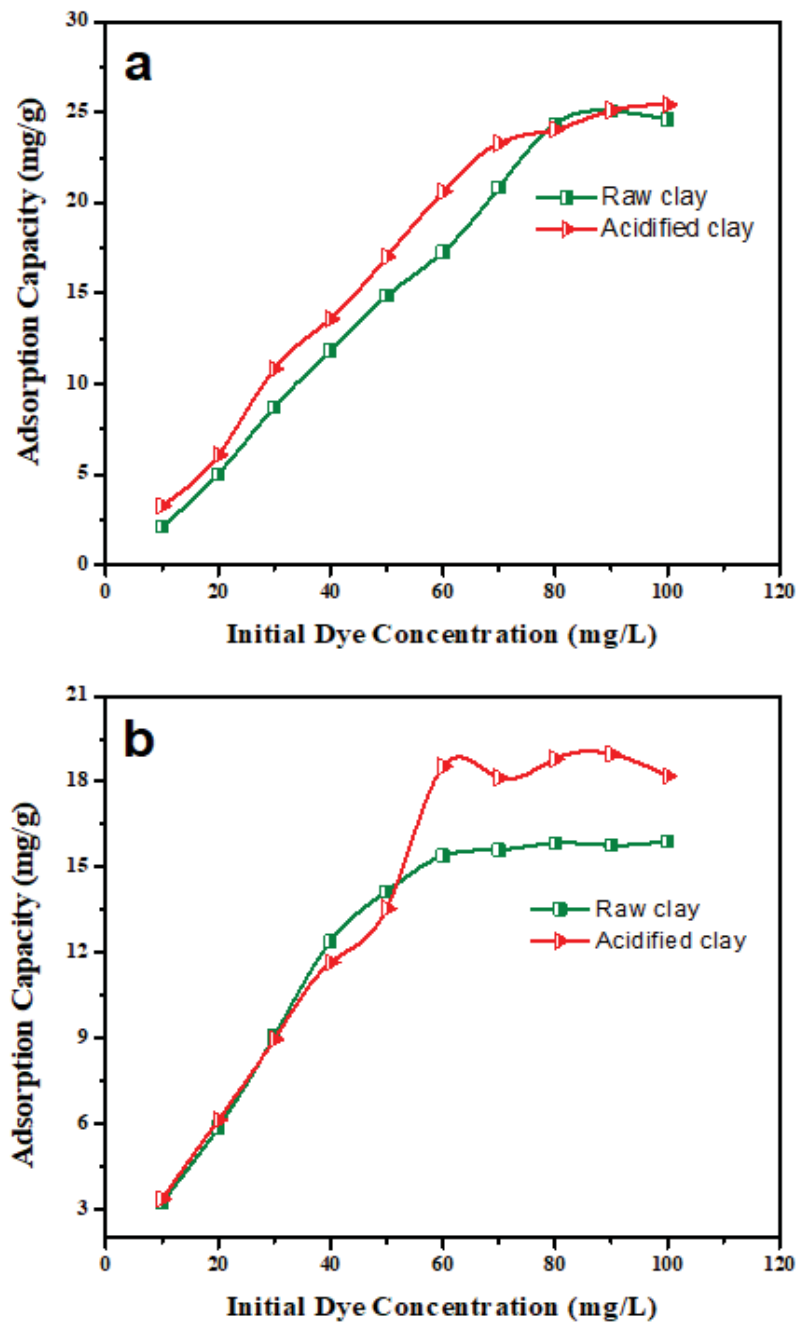
Fig. 9. Effect of initial dye concentration on the removal of dyes onto raw and modified clay; (a) BFBN dye and (b) RFRN dye.
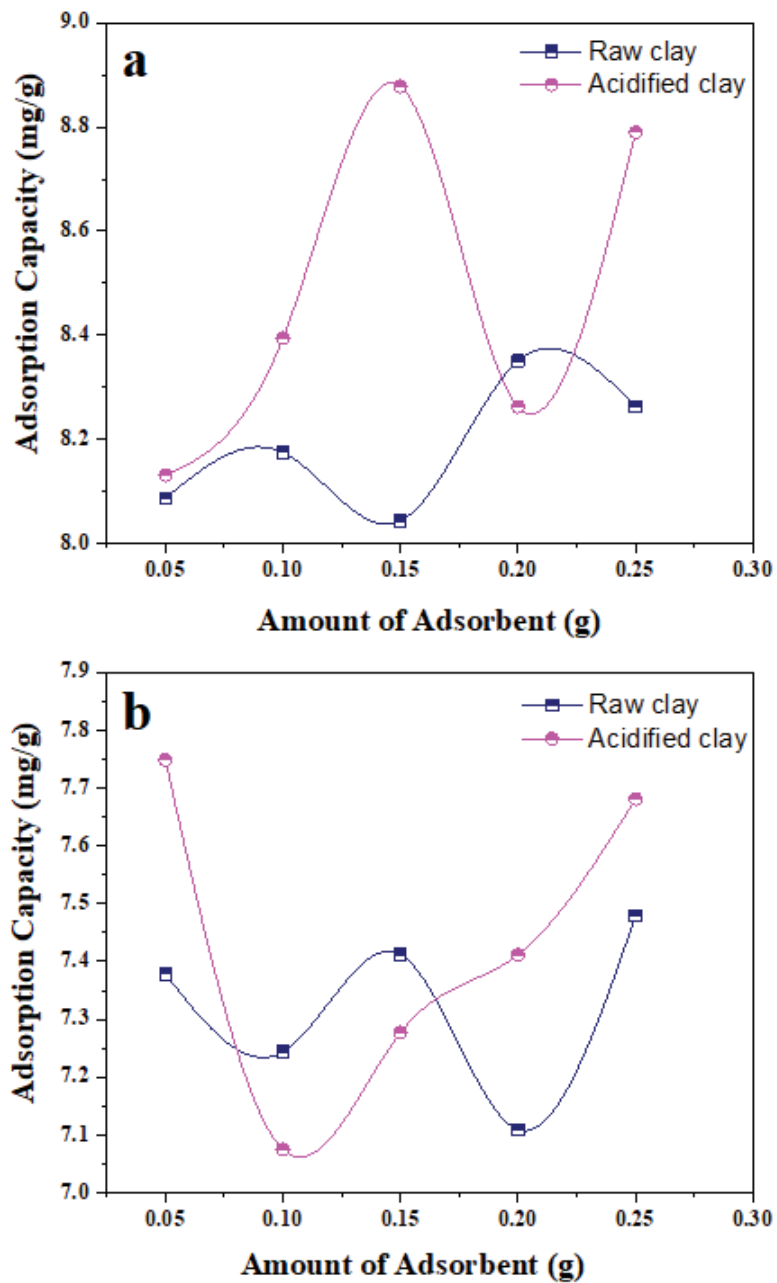
Fig. 10. Effect of adsorbent dose on the removal of dyes onto raw and modified clay; (a) BFBN dye and (b) RFRN dye.
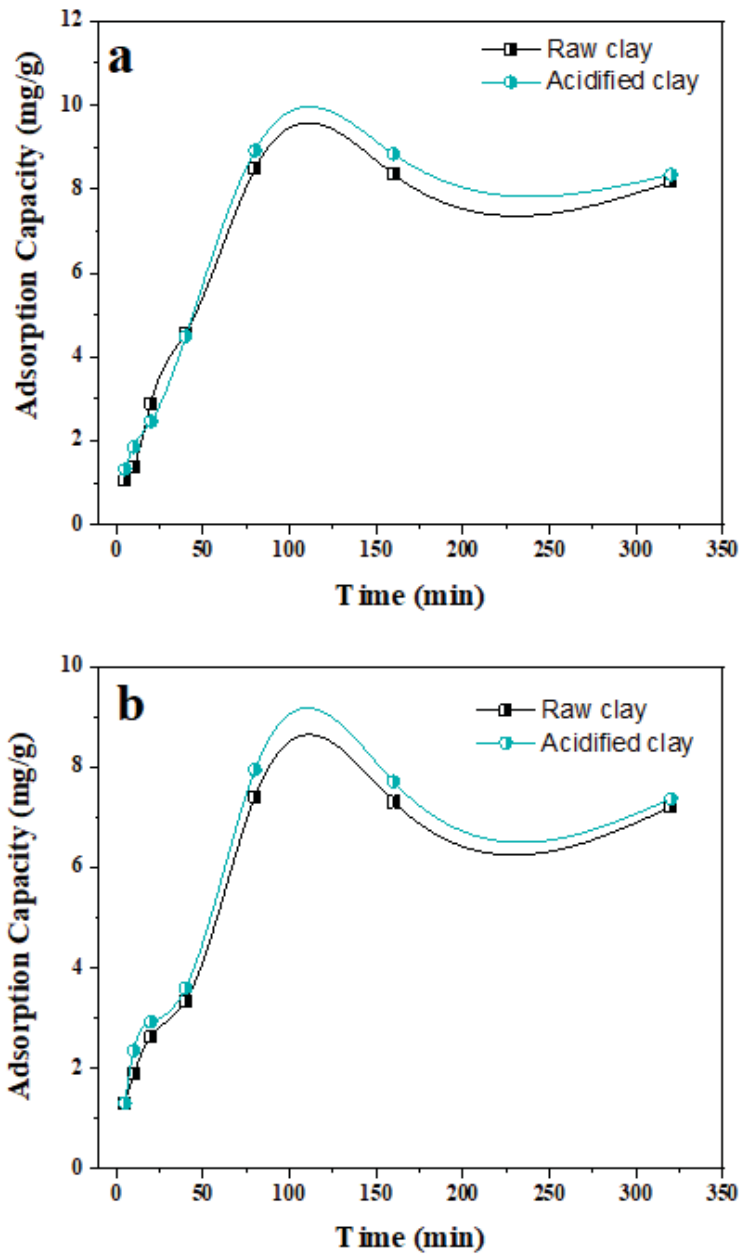
**Fig. 7.** Effect of contact time on the removal of dyes onto raw and modified clay; (a) BFBN dye and (b) RFRN dye.
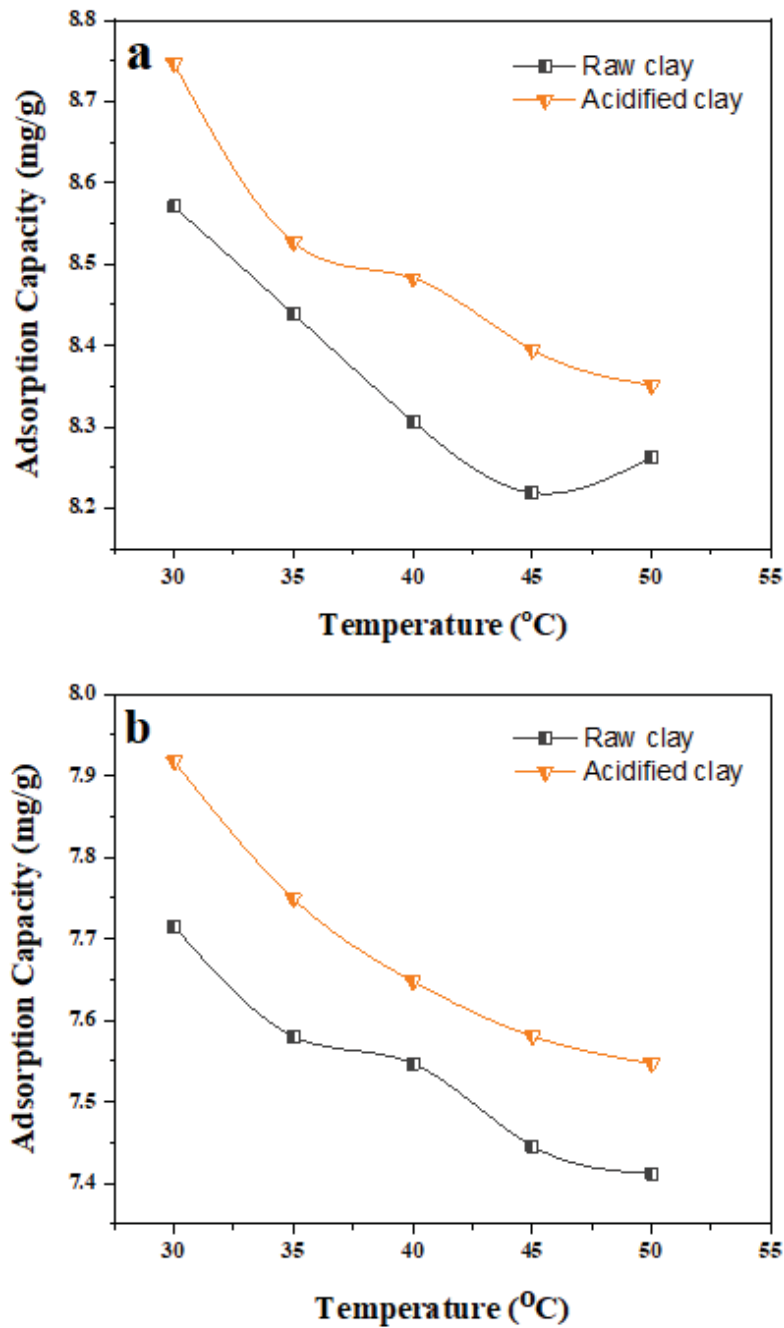
Fig. 8. Effect of temperature on the removal of dyes onto raw and modified clay; (a) BFBN dye and (b) RFRN dye.
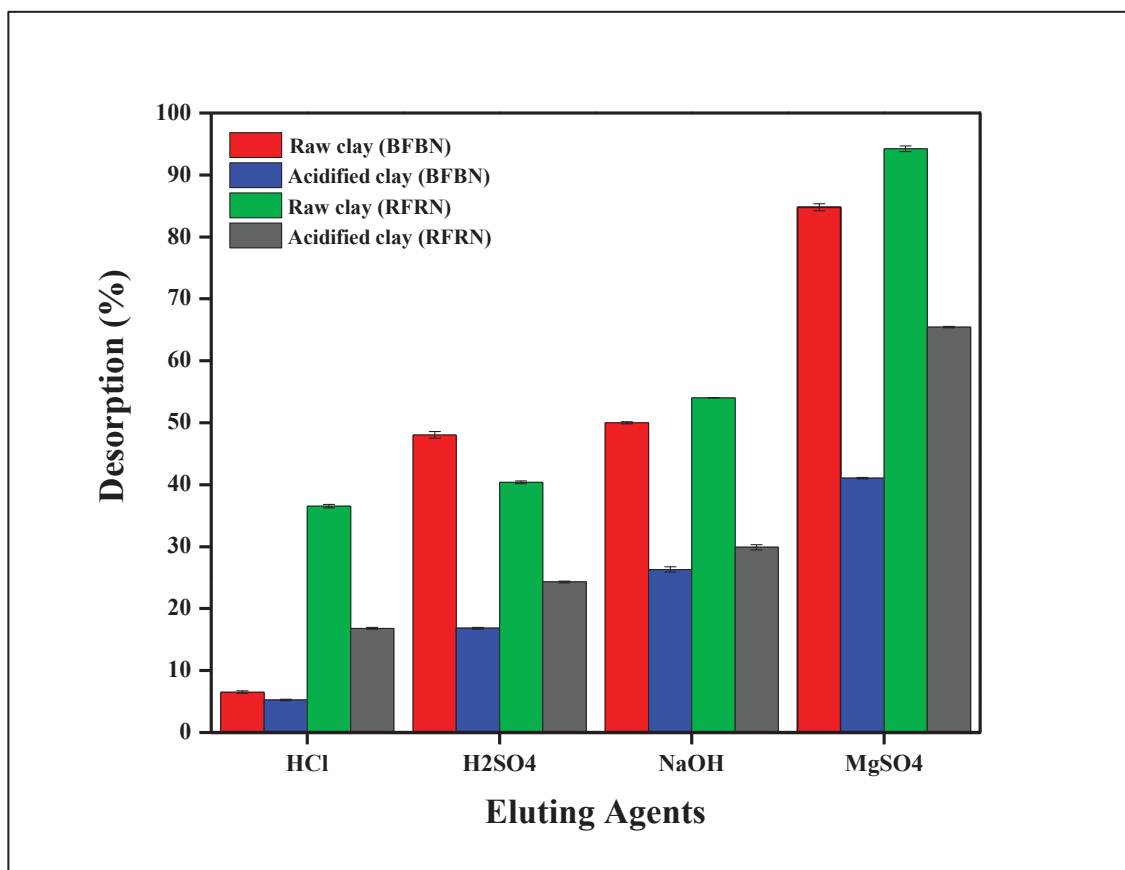
Fig. 9. Desorption of BFBN and RFRN dyes from raw and modified clay using different eluting agents.
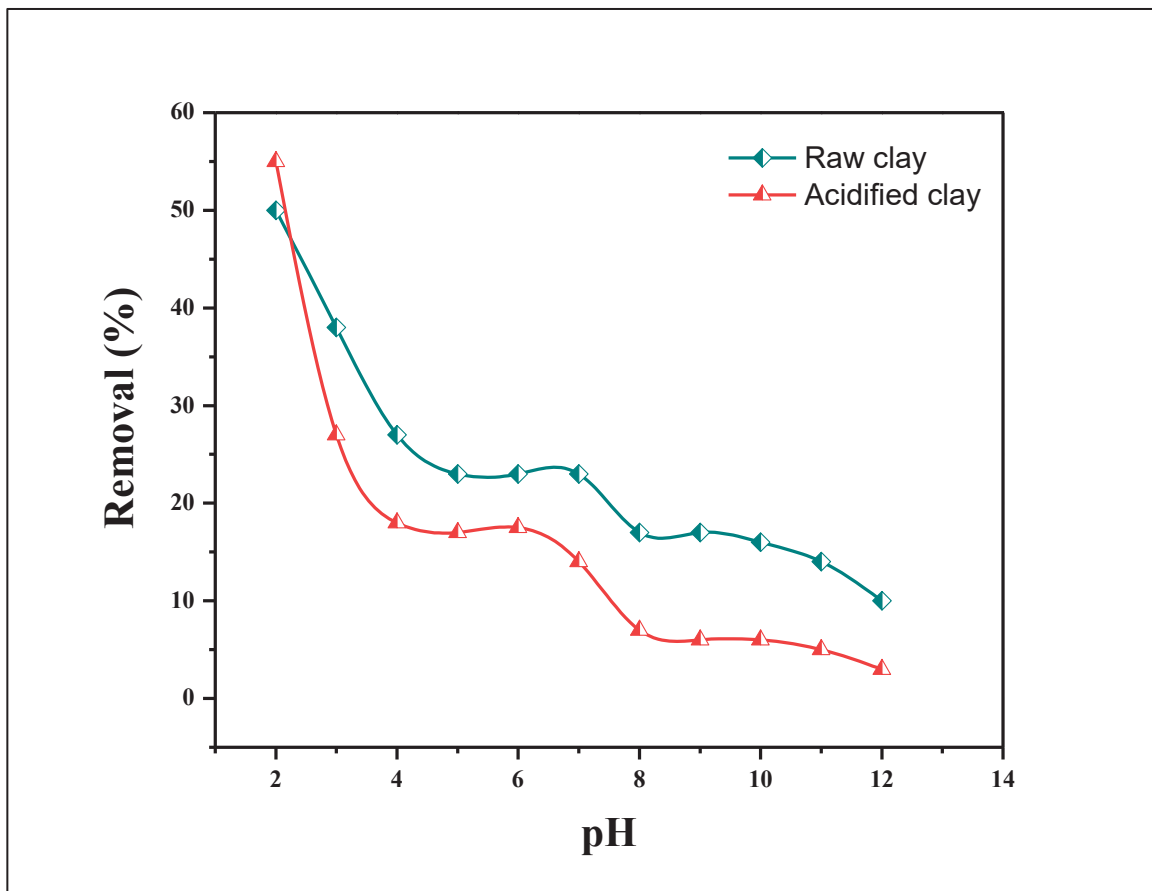
Fig. 10. The percentage removal of colour of textile effluents at different pH values using raw and modified clay.